CATÓLICA
ESCOLA SUPERIOR DE BIOTECNOLOGIA
PORTO

MICROPATTERNED SILK FIBROIN MEMBRANES FOR GUIDED TISSUE REGENERATION

by

João Alexandre Gouvinhas de Pina

November 2019

CATÓLICA
ESCOLA SUPERIOR DE BIOTECNOLOGIA
PORTO

MICROPATTERNED SILK FIBROIN MEMBRANES FOR GUIDED TISSUE REGENERATION

Thesis presented to Escola Superior de Biotecnologia of the Universidade Católica Portuguesa to fulfil the requirements of Master of Science degree in Biomedical Engineering

by

João Alexandre Gouvinhas de Pina

Place: Escola Superior de Biotecnologia da Universidade Católica Portuguesa (ESB – UCP) and Instituto de Investigação em Ciências da Vida e Saúde (ICVS)

Supervisor: Prof.ª Doutora Ana Leite Oliveira

Co-supervisor: Doutor António Salgado

November 2019

ABSTRACT

The role of tissue engineering in regenerative medicine has been evolving in the past decades, with biomedical technological developments allowing for an increasing number of medical applications. One of such developments has been to combine biomaterials with micropatterning techniques for guided tissue regeneration. In fact, studies have found that using biomaterials with micropatterned surfaces helps promoting cell growth and differentiation. Those results have generated high expectations regarding the treatment of worldwide impactful conditions such as spinal cord injury and periodontal disease.

Regarding these progresses and potential, this thesis looked towards assessing the hypothesis of using micropatterned silk fibroin (SF) membranes for applications in guided tissue regeneration. The membranes were produced by solvent casting and micropatterning was made via soft lithography by combining both microcontact printing (μCP) and microfluidic patterning techniques. The first objective was to obtain a controlled micropatterned topography in the SF membranes. Then it was important to characterize the micropatterned materials (MP) and compare their behaviour to non-patterned materials. MP displayed lower wettability, higher thickness and yet behaved equally in terms of mechanical performance. Finally, human derived adipose stem cells (hASCs) and periodontal ligament cells (hPDLs) were seeded on the different membranes to compare their capacity for cell adhesion and organization. Results showed successful adhesion and viability of both cell types to the membrane samples, particularly, in hPDLs samples, although cell organization was not observed in neither samples.

Keywords: Tissue engineering, guided tissue regeneration, micropatterning, biomaterials, periodontal disease, spinal cord injury.

RESUMO

O papel da engenharia de tecidos na medicina regenerativa tem vindo a evoluir nas últimas décadas devido ao desenvolvimento de novas tecnologias para aplicações médicas. De entre tais desenvolvimentos, a combinação entre biomateriais e tecnologias de micro padrões tem vindo a ganhar um papel de destaque na regeneração tecidual orientada. Estudos permitiram apurar que a utilização de biomateriais com superfícies micro padronizadas potencia o crescimento e diferenciação celular. Deste modo, estes resultados têm gerado grandes expectativas em relação ao tratamento de condições de impacto global, tais como lesão medular e doença periodontal (periodontite).

Com base neste potencial e progressos científicos, esta tese visou avaliar a hipótese de utilizar membranas à base de fibroína de seda (SF) com micro padrões para aplicação em regeneração tecidual orientada. As membranas foram produzidas através do método de *solvent casting* e os micro padrões foram conseguidos por *soft lithography*, combinando as técnicas de *microcontact printing* (μCP) e *microfluidic patterning*. O objetivo primário foi a obtenção de uma topografia com micro padrões específicos nas membranas SF. Seguidamente, caracterizaram-se os materiais com micro padrões (MP) e compararam-se com os materiais sem padrão, resultando na observação de menor molhabilidade e maior espessura em MP, porém o comportamento mecânico foi semelhante. Por fim cultivaram-se nas diferentes membranas, células estaminais de derivadas de tecido adiposo humano (hASC) e células do ligamento periodontal humano (hPDL), de forma a tecer a comparação entre as capacidades adesivas e de organização das células nos materiais. Os resultados foram bem sucedidos no contexto da adesão e viabilidade de ambos os tipos de células nas amostras de membranas, particularmente, no caso das amostras com hPDL, porém não foi possível observar-se uma organização bem definida em nenhuma das amostras.

Palavras-chave: Engenharia de tecidos, regeneração tecidual orientada, micro padrões, biomateriais, doença periodontal, lesão medular.

ACKOWLEDGEMENTS

The work presented in this thesis was partially performed in the Life and Health Sciences Research Institute (ICVS) Financial support was provided from Prémios Santa Casa Neurociências - Prize Melo e Castro for Spinal Cord Injury Research (MC-04/17). It was also funded by FEDER, through the Competitiveness Internationalization Operational Programme (POCI), and by National funds, through the Foundation for Science and Technology (FCT), under the scope of the projects POCI-01-0145-FEDER-007038; TUBITAK/0007/2014; PTDC/DTP-FTO/5109/2014; POCI-01-0145-FEDER-029206; POCI-01-0145-FEDER-031392; PTDC/MED-NEU/31417/2017 and NORTE-01-0145-FEDER-029968. This work has also been developed under the scope of the project NORTE-01-0145-FEDER-000013, supported by the Northern Portugal Regional Operational Programme (NORTE 2020), under the Portugal 2020 Partnership Agreement, through the European Regional Development Fund (FEDER). Therefore, I would like to express my deepest gratitude to ICVS for allowing me to work in its facilities and to make use of their equipment methods and knowledge. All of which were fundamental for the development of this thesis. On the same note, I cannot stress enough my gratitude towards Escola Superior de Biotecnologia da Universidade Católica Portuguesa (ESB-UCP) for my formation, both as an academic and personally. The memories and the people I take with me from my time spent in this university shall go on with me and within me.

There is not enough space – nor enough words - to describe how much I am thankful to all the people who have influenced and supported my work through the struggles and in the victories. It was because of those people that I never walked alone, felt demotivated or lacked confidence in pursuing my goals. I would like, however, to give my special thanks to a few people.

To Prof. Ana Oliveira, for her guidance, relentlessness, support and ever motivating spirit when everything seemed most difficult. For allowing me to be a part of her team and for making it seem as if everything could be done if my arms never laid down. For her optimism, for making me strive towards better goals, for investing in me and for her trust.

To Dr. António Salgado, for accepting me so fondly on his team and workspace, for gifting me with the amazing experience of working on the ICVS, where I acquired an amount of knowledge on neurosciences, by working in close proximity with it.

To Prof. João Paulo Ferreira, coordinator of the MSc programme of Biomedical Engineering, for the opportunity of my attending this Master of Science degree programme.

To Rita Silva, for her teachings and assistance, for worrying about my work and for investing in its progression. I would like to further express my gratitude towards her for her kindness, patience and for helping me become more competent and professional within an ambitious environment.

To Dra. Juliana from the Centre for Rapid and Sustainable Product Development of Instituto Politécnico de Leiria (CDRSP – IPLeiria), for her collaboration and enthusiasm in the development of the moulds used for this thesis.

To Prof. Rui Barros, Dra. Cassilda Reis, Dra. Ana Rita, Dr. Rui Magalhães and Ricardo Serôdio for their help, by the way of advices and different contributions to this thesis.

To my family, for all the love, motivation and the trust they had in me. For believing in my capabilities and potential. For all the stories and moments. For the traditions and for always sticking together as time moves on.

To my friends, to all of them, from all different backgrounds: the ones from childhood, the ones from university and the new ones. Their support and care throughout this year was fundamental. The jokes, laughs, and the arguments we have had played a part in making the moments we shared, memorable.

To my girlfriend, Ana. Words cannot describe how much of an influence she was through the course of this thesis. I am so very grateful for all the words of advice, support and love. For always being aware of any trouble I might have faced and for never letting me go down. For her faith in me, in my achievements and potential. For her companionship, maturity and wisdom. And lastly, for being so dear to me.

Last, but surely not least, I would like to thank my parents for their unconditional love, comprehension, patience, support and food. For their investment in me, not only financially, but mostly psychologically. For making it possible for me to go through with my studies. For doing the best they could to help and guide me. They have truly been my pillar of support. I would not be here if not for them.

TABLE OF CONTENTS

LIST OF FIGURES

LIST OF ABBREVIATIONS

CA – Contact angle

CTR – Smooth surfaced control membranes

DAPI - 4',6'-diamino-2-phenylindole

Gly – Glycerol

hASC – human adipose-derived stem cell

hPDL – human periodontal ligament-derived cell

MP – Micropatterned membranes

MTS – 3-(4,5-dimethilthiazol-2-yl)-5-(3-carboxymethoxyphenyl)-2-(4-sulfophenyl)-2H-tetrazolium

PBS – Phosphate buffer solution

PD – Periodontal disease

Pha – Phalloidin

RT – Room temperature

SCI – Spinal cord injury

SEM – Scanning electron microscopy

SF – Silk fibroin

SFE – Surface free energy

TE – Tissue engineering

I. INTRODUCTION

1. The concept of Tissue Engineering

Tissue engineering (TE) is a field that utilises materials and biological, biochemical and physical factors to build strategies for the creation of a wide variety of patient-specific treatments by improving, maintaining, restoring, regenerating or replacing a biological tissue [10]. For the last quarter of a century, tissue engineering has been dedicated to the development of new therapeutic solutions for the regeneration of different types of tissues, via manipulation of cells, biochemical factors and materials. In order to achieve such objectives, a symbiosis has been created, aligning this engineering branch with various life science fields.

Although TE is a very promising research field, the number of FDA approved materials that include biological components is still relatively low. In fact, in 2018, only a handful of approved strategies included a combination of cells with materials [29].

1.1. Medical relevance

Despite the reduced clinical application of TE, multiple studies aided by technological advances in the fields of molecular and cell biology have been conducted to develop treatments that stimulate regenerative processes, hence accelerating the healing of injuries and wounds in patients [20][26][59][78]. Most of these treatments rely on the use of grafts or on the production of tissues outside the body in an attempt to control its regenerative capacity [6][40]. The development of such tissues integrates the use of both natural or synthetic materials, which may feature biological elements to induce specific *in vivo* reactions and boost healing [29].

One example of these treatments relies on the utilization of naturally derived extracellular matrix (ECM) or by coupling growth factors with materials to induce the healing process [41][79]. Treatments like these have motivated further research on the use of biological elements in the regeneration of different types of tissue [38].

2. Micropatterning for guided tissue regeneration

Materials with patterned surfaces have been driving the attention of tissue engineers [47]. The use of such materials in the tissue engineering field holds a great potential in promoting highly defined cellular interactions which may, in turn, lead to better and controlled

tissue growth [12]. Consequently, the advancements in the technologies for the development of micropatterned materials have enabled the proposal of more specific and ambitious applications as different as: the creation of antimicrobial surfaces [47]; tissue regeneration [12]; and stem cell differentiation [74].

These applications, according to Thery, take advantage of how that animal tissue is formed, its architecture, the geometrical and mechanical implications of tissue growth and its impact on the surface morphology. Such is the case of muscle tissue, whose topographical display follows a straightforward pattern in result of the muscle fibres' alignment [74]. Thus, micropatterning stands as a tool for a better control of both cell growth orientation and differentiation [63]. However, the pathway towards producing efficient tissue growth-inducing micropatterned platforms relies on the kind of materials used.

The materials used in these applications, must fulfil the necessary requirements in order to enable efficient *in vivo* and *in vitro* responses according to the conditions set by the biological environment for such applications. For instance, the materials must be biocompatible, biodegradable and malleable for its use within a biological microenvironment and must also enable cell adhesion in order for its proliferation [74]. These characteristics are paramount to ensure optimal mechanical performance and to successfully promote cell adhesion and proliferation along the patterned surfaces of the material hence leading to the growth of new functional tissue [24].

Regarding those requirements, most studies in the matter have used membrane biomaterials as most befitting for both micropatterning display and guided tissue regeneration and have also been highlighted for their drug delivering potential [21][34][42][45][48]. These biomaterials would act as substrates for cell deposition after micropatterning was achieved, hence either translating the patterns on to the cells or accommodating the cells on their patterned layers [82].

2.1. Available micropatterning technologies

Novel available micro and nanoscale fabrication technologies have been highly contributing to achieve new knowledgement on cell behaviour. Nowadays, cell micropatterning and manipulation represent the standard for conducting experiments on drug testing, studying biochemical processes and designing devices for medical applications [49]. Moreover,

patterning techniques have proven to be invaluable for the understanding of interfacial interactions amongst cells and surface materials and also for cell differentiation and proliferation [62]. In fact, the control over cells and their layout via micropatterning techniques has enabled for cell-arrays to reproduce with satisfactory fidelity, authentic *in vivo* conditions [33]. Consequently, this has marked a significant evolution in TE, given the more accurate nature of 3D models in comparison to real animal tissue, both physiologically and metabolically [49].

Nowadays, considering the uncovered potentials of the micropatterning technologies and the refinement of technologies in general, many methods to fabricate patterns have been developed. Regarding TE and, most specifically, biomaterials and cell culture, the level of finesse required by the applications have led to the development and characterization of micropatterning methods specific for this field [17]. These methods involve physical and chemical processes in the fabrication of patterns and can be classified as direct (using addition or alteration of surface and materials, stencilling or even laser-guided writing) or indirect (with the use of stamps) [62].

Those methods are addressed in the following section.

2.1.1. Photolithography

This is a patterning method which consists of transferring geometric patterns from a mask on to a substrate by use of UV light [80]. The substrate is firstly coated with a photoresist on its surface, being then selectively exposed to UV light through a mask containing the wanted patterns. The patterns are then formed on the substrate which can then be used as a mask or as a master to the desired biological materials [62]. Next, the substrate is treated with a reagent, resulting in a cell adhesive and cell resistant micropattern. Afterwards, the materials can then be deposited on the surface and the remaining photoresist is lifted off, exposing the remaining areas which do not have biological material [80]. Photolithography has been held as a major method for producing patterns on solid surfaces, although its disadvantage falls upon the use of aggressive solvents to remove the photoresist which in turn may damage the biological materials and their binding to the surface [62].

2.1.2. Soft lithography

The method of soft lithography uses polymers to create stamps, which in turn replicate their micro or nanopatterns on to other surfaces, creating moulds out of these surfaces. Accordingly, this method stands as a more viable alternative for the creation of patterned materials due to the possibility of reutilizing the stamps and the moulds. Additionally, the samples produced can be observed directly by light microscopy [62]. As a result, soft lithography has become one of the dominant methods for micropatterning. In fact, different techniques have since been developed out of this method, them being: microcontact printing (μCP), microfluidic patterning and stencil patterning [80].

2.1.2.1. Microcontact printing

This technique, originally utilized for the patterning of gold, has since been applied by researchers in biomaterials. μCP consists of using a polymer stamp on a master mould (usually made of silicon) with an elastomeric material in it, as seen in Figure 1a. During contact between the stamp and the mould, the material is used to ink the stamp with a pattern. Next, after the ink has adhered to the stamp, it is left to dry and the pattern can then be transferred on to a desired surface by printing [4].

The process of creating a master mould can be time consuming due to the amount of time required for designing it. Nonetheless, researchers have been looking at the use of natural materials as a source for pattern design. For instance, a study used the vascular system of leaves to produce, with success, moulds for the growth of endothelial cells in the vascular patterns [81].

2.1.2.2. Microfluidic patterning

This technique works similarly to that of μCP although in here the patterning is obtained from a network of microchannels resulting from the pattern. Firstly, the mould with the patterns is put into contact with the substrate closing the microchannels of the patterns. Then, fluids can be poured onto the open edges of those microchannels and the biomolecules of the fluids are absorbed by the substrate to form the patterns (Figure 1b) [80]. This process makes microfluidic patterning an easier technique modulating a surface and benefits from not requiring a drying step [80].

2.1.2.3. Stencil Patterning

Stencil patterning requires thin sheets of polymeric materials (or stencils) containing different shaped and sized through holes (Figure 1c). The stencils are obtained in a similar fashion than that of the stamps used in μCP, by getting the polymeric material into contact with a master mould. Then, following the polymerization, the stencil is created after the peeling of the material off from the mould. Next, the stencil is put on top of the substrate leaving only the areas of the through holes exposed for the cells to latch on to substrate. Finally, once the stencil is removed, the cells would have made patterns shaped like the through holes [80].

This technique is, therefore, a simple one to exert and that does not require any kind of chemical alteration of the substrate. However, it is very sensible as the stencils are very delicate and may be damaged upon removal from the mould and from the substrate [80].

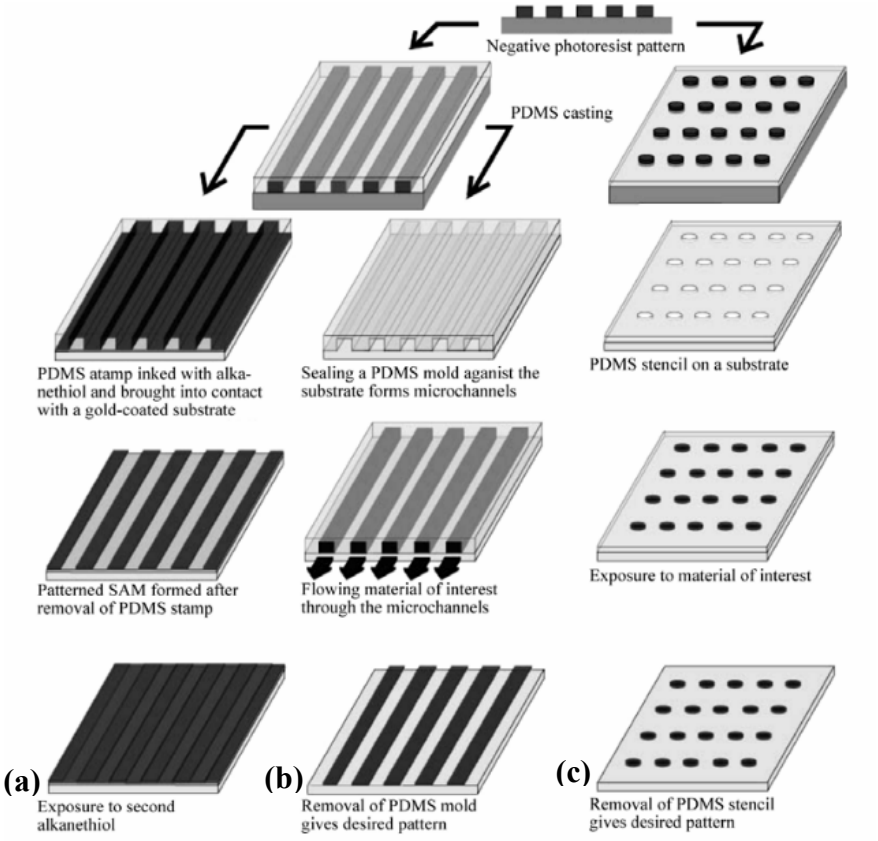

Figure 1. Schematic representation of soft lithography techniques: (a) microcontact printing, (b) microfluidic patterning and (c) stencil patterning. Polydimethylsiloxane (PDMS) is the polymer used to make the stamps. Adapted from [80].

2.1.3. Other technologies

Different means to achieve cell micropatterning not involving biomaterial substrate patterning are also available, as per previously mentioned. Those technologies though, make use of rather more direct approaches for micropatterning by manipulating the special behaviour of the cells. One of the ways to ensure such manipulation is directly positioning the cells into the desired pattern. Technologies that are based on this method are: ink-jet printing [75] and laser guided direct writing [62].

Ink-jet printing consists of an ink solution to create droplets holding cells. A piezoelectric dispenser device then prints out the droplets in a desired oriented array, generating a micropattern [49][75]. In laser guided writing, a stream of cells is delivered by an infrared laser beam which can be controlled to deliver the cells in a chosen orientation [49]. It can be also used for creating tissue by forming layers of cells, yet the laser might endanger the cells hence improvements to this technology are still necessary [17]. Either one of these technologies can also be used in indirect patterning to print out attachment factors such as proteins, in a surface, to promote cell adhesion and alignment [17].

Other existing technologies resort to physical methods for manipulating cell orientation. These micropatterning technologies such as acoustic force patterning and dielectrophoresis also stand out as direct approaches [49]. Acoustic force patterning consists of employing surface acoustic waves composed of electrodes on piezoelectric substrates, following their excitement. Next, the cells deposited on the same substrate migrate by influence of the acoustic nodes. The layout of the cells can thus be controlled depending on the type of electrode used, the intensity of the acoustic waves and the physical attributes of the cells used [49][55]. In the case of dielectrophoresis, electrokinetic forces and hydrodynamic effects are used to force the cells to move. In short, an electric field is applied in a substrate to induce a dipole moment which, depending on the polarity and permittivity of the cells and their medium, causes the cells to react by attraction or repulsion towards the electric field [32][73].

These technologies have proven to be promising as their positive *in vitro* test results demonstrate their potential for selective tissue regeneration and controlled cell differentiation [62]. However, their use can not only be limiting, as some of them might require external power sources and large instrumentation with complex setups, but also challenging due to the physical and chemical properties involved in the processes [49].

3. Therapeutic applications

The research in the tissue regeneration field focused on biomaterials and the addition of micropatterned characteristics have branched into different types of applications, with several developments focusing on micropatterned membranes [15].

For instance, regarding the muscle tissue, there have been tests using membranes to regenerate skeletal muscle tissue [64] and cardiac muscle tissue [36], but also micropatterned collagen membranes have been used to promote skeletal muscle tissue growth more recently [15]. The outcomes of these studies have all been successful, further validating the potential of the combination of these technologies.

Connective tissue has also been a target for studies with the use of osteopromoting membranes being used in bone tissue regeneration [43]. Furthermore, micropatterning has been used in regard to soft connective tissue [50][58]. In case of nervous tissue, there have been experiments also validating the use of membranes and micropatterned membranes to promote the growth and differentiation of this type of tissue [83][84]. This wide range of applications has, therefore, increasingly propelled these technologies for a potential use in the clinical field thus coming up as promising treatment options [29]. Applications in spinal cord injury and periodontal disease are very different on what concerns the biomaterial specifications, yet they can both benefit from the use of membrane systems and micropatterning. Therefore, these were explored in the present thesis.

3.1. Spinal Cord Injury

Spinal Cord Injury (SCI) is considered to be one of the most devastating central nervous system injuries [44]. The worldwide incidence rate of this condition has been on the rise in recent years, with epidemiological studies estimating 20 to 30 new cases in each million individuals, annually [46]. These numbers are most concerning, for there are no efficient forms of treatment available yet and the injury can result in both permanent voluntary motor dysfunction and the loss of sensation. This condition therefore constitutes a great economical and psychological load to the patients and their families [44][46].

SCI comprehends two main episodes, the primary traumatic damage and the chronic secondary damage, respectively [44]. The early stage of SCI consists of a traumatic injury to the spinal cord (as a result of a contusion injury, usually) leading to the rupture of its tracts,

which has been associated with an impairment of the neurological functions and deficiencies in the axon regeneration process. Next, the second stage comes associated with a series of complications that further impact the spinal cord tissue, such as oxidative stress, infiltration of inflammatory cells and inner haemorrhage. These complications are represented in Figure 2 [2].

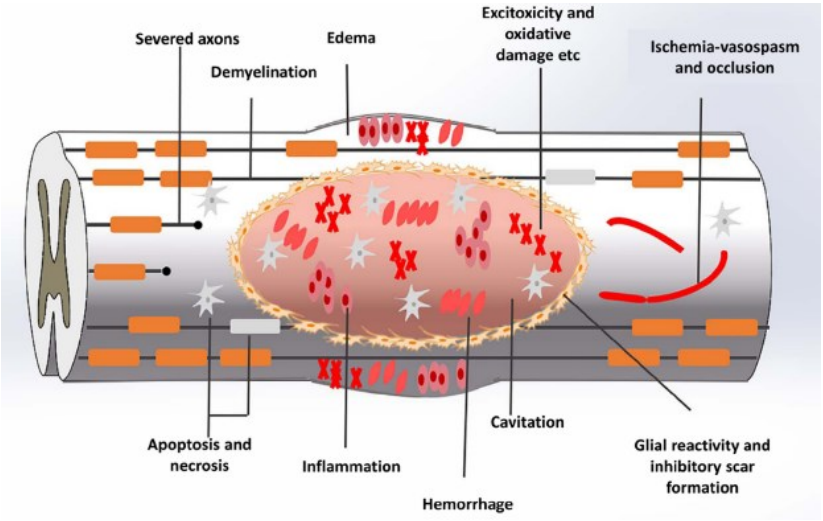

Figure 2. The pathological and physiological impact of spinal cord injury (SCI). Adapted from [44].

This chain of events is henceforth responsible for the generation of a toxic microenvironment that suppresses nerve regeneration [44]. Additionally, as a result of the neuronal dysfunction from the SCI, patients may see themselves at a higher risk of suffering from hypertension, nutritional dysfunction, systemic inflammation and reductions in lean body mass which may, in term, lead to an imbalance of energetic expenditure contributing to a state of obesity and prevalence of type-two diabetes mellitus and cardiovascular disease [18].

The impact caused by SCI is undoubtedly concerning and despite of the lack of effective treatment, this has only fuelled the ambition to research for viable options. Research on the topic began by recognising which growth inhibitors were present in the injured tissue to facilitate their modulation and thus promoting functional regrowth and enhancement of its regenerative capacity [46]. Other strategies include providing a regeneration support and guidance by using neural scaffolds or membranes and combining them with cells, drugs and other neurological factors [44]. This would require the membranes to have similar physical, chemical and microenvironmental qualities to those of the spinal cord tissue in order to create

a bridging effect between the new transplanted cells and those of the existing tissue. In the end, cell growth differentiation and orientation would allow for the regeneration of the damaged tissue [46].

These strategies have had their potential being explored and put into practise, with positive results coming out of the experiments. For instance, in 2013, agarose scaffolds with microchannel structures were produced and implanted in rats, with the results then indicating that the implants had helped guiding neural pathway regeneration after SCI [22]. In 2016, researchers implanted type I collagen membranes with identical structural characteristics of the spinal cord tissue into a rat with SCI [70]. The outcome demonstrated that the membranes promoted nerve repair by reducing the recruitment of phagocytic cells during both stages of SCI. In another study, tussah silk-based fibre scaffolds were used to test the *in vitro* treatment of spinal cord injured tissue, resulting not only in the observation of the compatibility with the mechanical properties of the tissue but also that the immune system did not reject the implants [77].

A more recent study used micropatterning technologies to arrange periodontal ligament cells in extracellular protein patterns with the cells being studied for their changes to their morphology, cytoskeleton, proliferation and differentiation. In the end, results showed that both the cells and their nuclei were elongated, whilst maintaining nuclear volume. Moreover, inhibition of osteogenesis and adipogenesis was observed, although micropatterned samples had an increase of collagen expression which provided insights into the resourcefulness of micropatterning for periodontal ligament tissue regeneration [87].

3.2. Periodontal disease

The Periodontal disease (PD) is a multifactorial chronic condition of the periodontum, in the oral cavity, characterized by the detachment of the junctional epithelium from the tooth surface and by the disconnection of the periodontal ligament fibre from the root cementum surface, resulting in the destruction of the surrounding alveolar bone. Figure 3 schematizes the early stages of this disease; whose evolution causes a progressive attachment loss of the periodontal ligament to the teeth ultimately resulting in their loss [56].

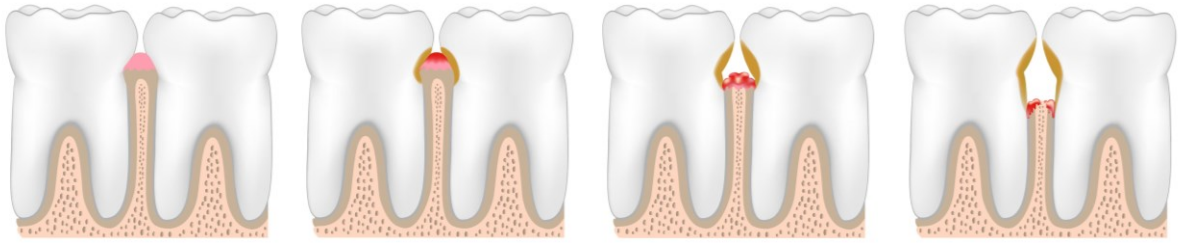

Figure 3. The evolution of the Periodontal disease (PD) from a healthy state (to the left) to a more progressive state (to the right). Adapted from [28].

The manifestation of this disease, however, may take on different forms according to its severity and the causes behind it. For instance, it may be manifested as periodontitis, aggressive periodontitis, chronic periodontitis or refractory periodontitis and its cause may be due to risk factors as different as the personal oral hygiene, smoking, mixed microbial infections, stress, obesity and type-two diabetes mellitus [3]. Additionally, it has been considered that PD may be associated with a wide array of systematic conditions such as the cardiovascular disease or cancers and that those conditions combined with PD could aggravate each other (Figure 4) [54].

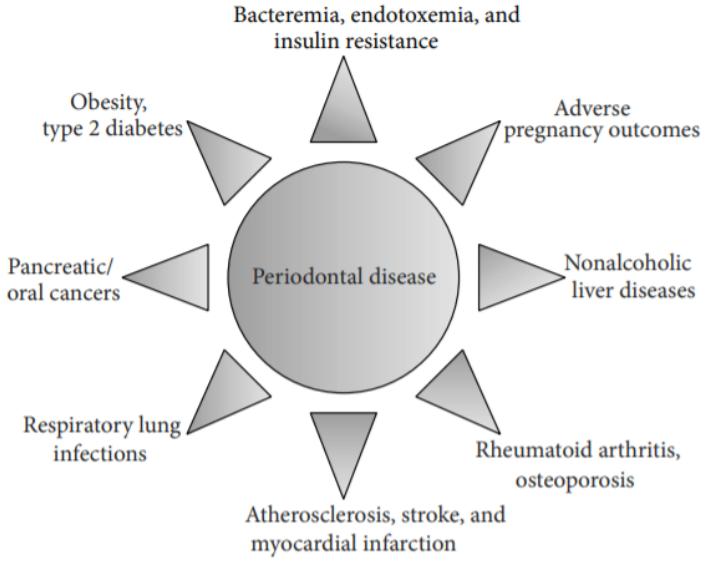

Figure 4. Diagram of health complications related to periodontal disease (PD). Adapted from [54].

The disease is considered to be one of the biggest threats to oral health with worldwide incidence rates estimated to affect up to 90 % of population [87]. In regard to these numbers

and by considering the many existing risk factors, the World Health Organization has been keen on emphasizing the importance of prevention of the PD by raising awareness to the factors that can me contained and managed. The practise of good oral hygiene, good dieting habits, stress management and quitting smoking come as examples of what can be done by the population in order to prevent the disease from developing [56].

In relation to treatment strategies, TE methods have been showing promise in tackling the issue by inducing periodontal tissue regeneration through a combination of biomaterials, growth factors and cell-based therapy. In fact, studies have fixated on whether topographical features may be of influence to the structural and functional attributes of periodontal-like tissue in guided tissue regeneration [61]. However, given the complexity of the organization of this kind of tissue, there is still much need for an optimization in the fabrication of multiphasic biomaterials to regenerate and reproduce the structural integrity of the multi-tissue interface [61]. Nevertheless, current available advancements in topographical technologies have allowed for the fabrication of scaffolds that facilitate the control of multi-tissue organization and positioning [27][72]. For instance, a research was made to assess the capacity of some developed polycaprolactone (PCL) scaffolds, with micro and mesoscale topographical attributes, to form aligned bone-ligament-cementum complexes *in vivo*. The results of that study saw an increase of tissue alignment and of oriented collagen fibre thickness as well as an overall cell alignment and nuclear elongation. Additionally, it proved that scaffolds with both micro and mesoscale topographical attributes can be used to align cells for oral tissue restoration and that they have the potential to improve regenerative response of multi-tissue complexes [61]. In another research, a combination of PCL micropatterned scaffolds with controlled growth factor gene delivery and cell-based therapy was accomplished. Then, it was seeded with human cells for implantation on rats with large alveolar bone defects, resulting in enhanced bone formation due to gene delivery system. Also, it was observed that the micropatterning promoted the regeneration of ligament tissue similar to periodontal ligament [60].

II. OBJECTIVES

In the present thesis micropatterned membranes based on silk were developed for applications in guided tissue regeneration. Solvent casting was used in order to produce membranes with patterned channels with adequate spacing for cell alignment and guidance, without compromising its mechanical and physicochemical properties. Two different cell sources were used, human derived periodontal ligament cells (hPDLs) and human derived adipotic stem cells (hASCs) to evaluate the potential of these engineered surfaces in applications such as periodontal regeneration.

III. MATERIALS AND METHODS

1. Reagents and materials

1.1. Reagents

All the reagents used in this work were purchased from Sigma-Aldrich, St. Louis, United States of America, unless otherwise stated.

1.2. Silk material

Silk is a fibrous protein produced by different types of insects who use it for a wide range of purposes such as protection, mobility and to capture other insects [85]. The silkworm *Bombyx mori* is the most commonly used silk-producing specie and has, therefore, been widely used commercially in biomedical applications and in the textile field [5][71]. The use of silk as a biomaterial is attributed to its optimal mechanical properties, biocompatibility and malleability [71][76]. Studies have also proven silk to be biocompatible and non-toxic, being even degraded and absorbed via proteolytic action, over time [5].

These properties are a result of the β-sheet conformation of silk caused by its constituting proteins: sericin and fibroin. The semi crystalline structure of fibroin enables it with interesting qualities such as strength, stiffness and resilience. On the other hand, sericin, structurally non-crystalline, is responsible for maintaining the integrity of the silk fibre, as it

sheaths the inner-located fibroin. These proteins can be separated by a degumming process in which sericin is removed, leaving behind fibroin fibres [51].

The structure of the material enables the use of silk-based products for biomedical applications in the tissue engineering field, with a diversity of applications such as the production of scaffolds [5], coatings [76] and drug delivery mechanisms [30].

In the present thesis silk was used for the production of the membranes from *Bombyx mori* cocoons provided by the Portuguese Association of Parents and Friends of Mentally Disabled Citizens (APPA-CDM), Castelo Branco, Portugal.

1.3. Silk fibroin-based solution preparation

Bombyx mori cocoons were clean and cut into small pieces that were boiled for 1 hour in 2.00 L of a 2.12 g/L solution of sodium carbonate. This step ensured the extraction of the sericin from the silk fibroin (SF). The obtained SF fibres were washed by boiling for 30 min in 1.00 L of distilled water after which the fibroin was left to dry for 48 hours at room temperature (RT). Dried SF meshes were dissolved in a 0.81g/mL saturated solution of lithium bromide (Honeywell, UK) during 2 hours at 70 ºC. Next, the lithium bromide present in the resulting solution was removed, through a dialysis process against 5.00 L of distilled water for 48 hours during which the water was changed 12 times. This step was accomplished using benzoylated tube membranes composed of regenerated cellulose, with 9 mm width and pores with molecular weight cut-off of 2000 Da. These tubes allowed for the lithium bromide to be released whilst water entered the tubes in its place. Then, the solution was filtered to remove any residual impurity and kept in the fridge at 4 ºC for further use.

Glycerol (Gly) was then added to the SF solution in a 1:4 ratio. Gly is one of the most versatile chemical substances, derived from natural and petrochemical sources, having low toxicity. In aqueous solutions, Gly is stabilized by intramolecular hydrogen bonds and intermolecular solvation of the hydroxyl groups, acting as a plasticizer [11]. Therefore, it is widely used in the production of films and membranes to decrease the brittleness whilst increasing elasticity and malleability [65].

2. Production of silk fibroin membranes

The SF membranes were produced through a method called solvent casting [23]. This method consists of dissolving a polymer - in this case, SF water-based solution - in an organic solvent, followed by the casting of this solution in a master mould and by its drying, thus releasing the solvent and resulting in a membrane.

2.1. Fabrication of moulds for micropatterning

The first objective of this thesis was to produce membranes with the capacity to promote cell adhesion, enabling their growth along an oriented pattern. This pattern required specific dimensions that should be wide enough for cells to settle in but narrow enough to prevent a concentration of cells within the same area. Furthermore, as the targeted cells to be used in this study were eukaryotic animal cells and since their average size varies between 10 µm and 100 µm [57], the patterns on the moulds were required to be made up of grooves of the same dimensions.

The pattern used was from a long play (LP) vinyl record and the method used to create the master mould from the record's micropatterns was soft lithography, more specifically microcontact printing (µCP). The vinyl record disc was used as the micropattern template for the mould, as its average width for the grooves was around 40 µm and 80 µm at half-way up the wall of the groove [1]. When cut into a circular-shaped piece with size of a regular petri dish (10.0 cm in diameter), the grooves on that piece were nearly straight, as presented in Figure 5.

Figure 5. Example of a vinyl piece used to generate the patterns in the moulds.

The moulds were produced of silicon Koraform A42 A and its respective catalyser (Koraform A42 B) in a 10:1 proportion. The production of the moulds was performed at the Centre For Rapid and Sustainable Product Development of Instituto Politécnico de Leiria (CDRSP – IPLeiria) and one such the moulds can be observed in Figure 6.

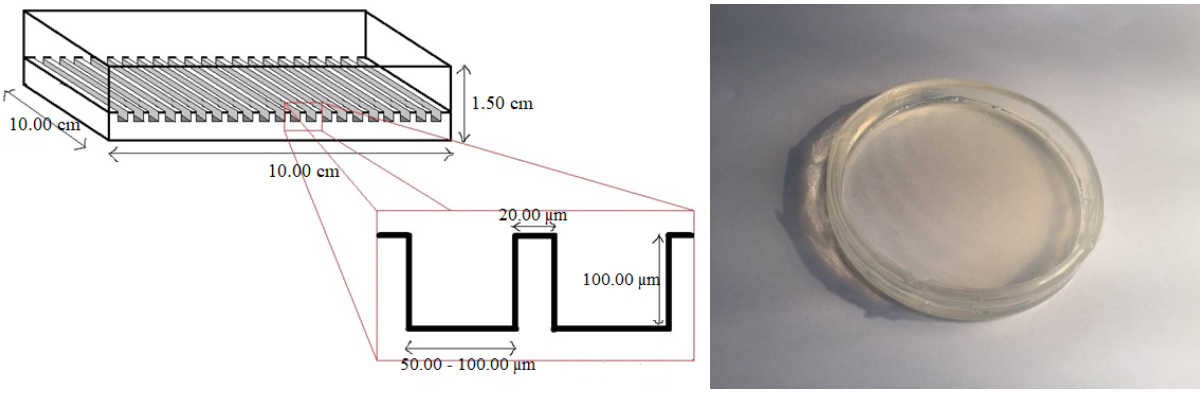

Figure 6. Initial layout for the moulds and their micropatterned grooves (on the left) and Micropatterned mould developed at Instituto Politécnico de Leiria (on the right).

2.2. Casting, drying and crystallization

The micropatterns from the mould were reproduced in the membranes by using another soft lithography method, microcrofluidic patterning. For this method the SF/Gly solution was poured into the micropatterned moulds but also into surfaced petri dishes (diameter 8,700 cm) (10,00 mL of solution per mould and petri dish) to produce the micropatterned (MP) and control (CTR) membranes, respectively. The membranes were left to dry at RT for 72 hours, where the SF solution solidified according to the topography present. After the drying period the membranes were detached from both the moulds and transferred to petri dishes, where they underwent a water annealing process. This step was required to induce the crystallization of the membranes into a water-stable conformation (beta-sheet, silk II) while serving as a sterilization process prior to cell culture [31]. In this process the membranes were immersed in a 70% ethanol solution (70% absolute ethanol plus 30% deionized water) for 2 hours, after which they were washed with and kept in a phosphate-buffer solution (PBS) solution and stored.

3. Characterization

3.1. Morphological analysis by Scanning Electron Microscopy

Scanning Electron Microscopy (SEM) analysis was performed at the Instituto Politécnico de Leiria, using a SEM Vega-3-LM (TESCAN, USA), to evaluate the morphology of the micropatterns on the surface of the membranes and to assess how the micropatterned grooves were arranged in the surface of the membrane. Prior to the analysis, the samples were coated with Au/Pd in a sputter coater by Quorum Tecnologies to improve the quality of the information collected.

3.2. Surface wettability and free energy by water contact angle

The wettability of a surface is an important feature when studying biomaterial-cell interactions. This property is a result of both the contact angle (CA) between the surface and a liquid and of the surface free energy (SFE) according to the nature of the surface [8]. The CA and SFE results were acquired by a goniometer equipment, Attension Theta (Biolin Scientific, Sweden) (Figure 7), using the sessile drop methodology. In this method, a video was recorded of a water drop on 1 cm x 3cm strip samples of the CTR and MP membranes whilst the CAs were measured from those images using OneAttension software by Biolin Scientific containing an algorithm fitted to that purpose.

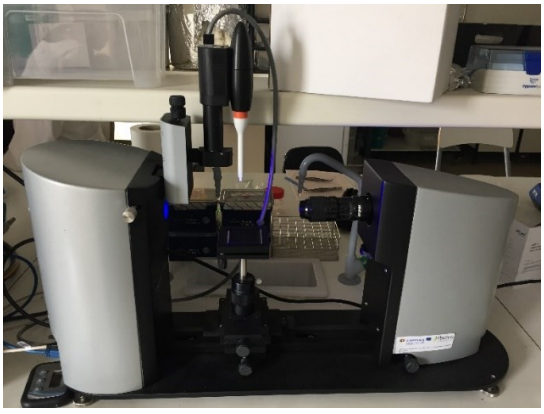

Figure 7. Goniometer used for sessile drop method.

The CA represents the angle between the tangent of the liquid-vapor interface and the solid surface (in this case, the strips) at the three-phase contact line (Figure 8) [8]. The CA is measured between the liquid used for the test and the solid surface, conventionally, and has been characterized according to the Young equation:

$$\cos\theta_{Young} = \frac{\gamma_{sv}-\gamma_{sl}}{\gamma} \quad (1)$$

Here, the θ_{Young} consists of the Young contact angle, γ_{sv} and γ_{sl} are the solid-vapor and solid liquid SFEs, respectively, and γ is the SFE of the liquid. According to the equation, a solid surface with high surface energy presents a tendency to display a low CA, while a low-energy surface tends to show a high CA [8].

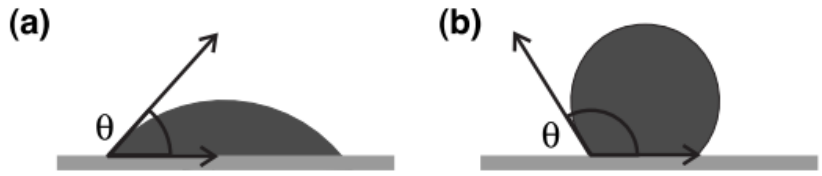

Figure 8. Schematic representation of the contact angle θ between a drop and a solid hydrophilic surface (a) or a hydrophobic surface (b). Adapted from (Ryan & Poduska, 2014)

The calculations of the SFE were performed using the OneAttension software as well, which then presented the results according to different methods: the equation of state, OWRK/Fowkes, Wu and Zisman. However, the equation of state, unlike the other methods, requires only one liquid for the test and does not divide the SFE into different components. This, coupled with the fact of its formula being controversial as to whether some of its elements are universal constants or outcomes of iterative processes, makes this method not as reliable as the others. On the other hand, the Zisman method requires the usage of more than just two liquids in order to offer more consistent results [8].

Thus, the OWRK/Fowkes and Wu are the most reliable methodologies as they consider the division of the SFE into independent components associated with different interactions and when combined with the Young equation it enables the assessment of the SFE. In the OWRK/Fowkes method, the resulting equation works as a geometric mean whereas in the Wu method, the equation works as a harmonic [8]. Both of these methods use for their equations two liquids with known dispersive and polar components in order to solve them, with one liquid

measuring the polarity and the other measuring the dispersion. In this study, water was used as the polar liquid given to its dominant polar component whilst diiodomethane was used as dispersive [8].

The results were expressed as the average of 3 measurements for each type of condition ± standard deviation.

3.3. Mechanical characterization

The determination of the mechanical properties of the membranes was achieved via uniaxial tensile tests, using a TA.XT Plus Texture Analyser (Stable Micro Systems Ltd., Surrey, United Kingdom) with tensile grips (Figure 9).

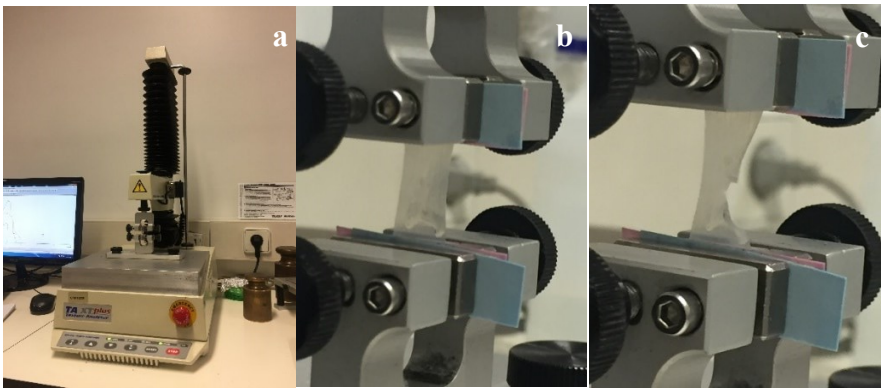

Figure 9. TA.XT Plus texture Analyser setup (a) CTR sample positioned in tensile grips ready for testing (b) CTR sample after reaching breaking point (c).

In this study, the samples consisted of 5 replicates of 1cm x 3cm strips for each CTR and MP membranes that were tested at a dry state and at a hydrated state which was the result of a 2-hour immersion of the samples in PBS. To setup the software of the texture analyser, it was required that the thickness of the samples was measured in beforehand so that the settings of the equipment as well as the results of the tests were best fitted for the characterization. The measurement of the thickness was performed in a micrometer MI20 (Adamel Lhomargy, France) [86].

Additionally, to achieve a better and steadier grip by the equipment, thin cards were attached to the edges of the samples using double sided adhesive tape. The samples where then

placed between both tensile grips which stood at 10 mm from each other, all the while the test speed was set to 25mm/min, with a trigger force and break sensitivity of 5g each [86]. After each test, experimental typical stress-strain plots were obtained, which allowed for the calculation of:

- Young's modulus (E), or modulus of elasticity, which describes the elastic properties of a material undergoing stress and deformation and is therefore characterized as the slope of the stress-strain curve;
- Ultimate Tensile Strength (UTS), which can be calculated by:

$$\text{UTS (MPa)} = \frac{\text{Maximum load (N)}}{\text{Cross sectional area (mm}^2\text{)}} \quad (2)$$

- Strain at tensile strength, characterizes the deformation demonstrated by the sample upon reaching the maximum tensile strain and can be determined by:

$$\frac{\text{Initial sample length (mm)-Sample length at maximum tensile strength (mm)}}{\text{Initial sample length (mm)}} \quad (3)$$

- Stress at break, which stands as the force applied on the sample per unit of area at the moment of break:

$$\frac{\text{Force at break point (MPa)}}{\text{Area (mm}^2\text{)}} \quad (4)$$

- Elongation at break (ε), calculated by:

$$\varepsilon\ (\%) = \frac{\text{Sample length at break (mm)-Initial sample length (mm)}}{\text{Initial sample length (mm)}} \quad (5)$$

- Offset yield stress, defined as the stress that makes the sample assume a plastic deformation which occurs upon reaching the yield point, or the moment when the material starts deforming nonlinearly;
- Strain energy, the amount of energy absorbed by the material up until its breaking point also described as the area under the stress-strain diagram.

For the purpose of discussing of these tests, the more relevant parameters, according to the practical objectives of these membranes, for the characterization of the samples are the Young's modulus, ultimate tensile strength and the elongation at break [19][23]. All other parameters are dependent from these and thus their discussion was not required.

4. Cell culture

4.1. Cell source

The cells used in this thesis were chosen based on the potential clinical application of micropatterned membranes in guided tissue regeneration for the treatment of periodontal disease and SCI.

Therefore, it was necessary to study the behaviour of cells with similar attributes as the target tissues. In the case of periodontal disease treatment, human periodontal ligament-derived cells (hPDLs) were used whilst for the treatment of SCI, human adipose-derived stem cells were chosen.

4.1.1. Periodontal Ligament Cells (hPDLs)

Human periodontal ligament-derived cells (hPDLs) are fibroblasts that produce connective tissue in the periodontal ligament, which is responsible for maintaining the teeth attached to the alveolar bone and to the gingiva. The need for these cells to align and organise themselves to form a stable and strong tissue, makes micropatterned surfaces a highly suitable technology for application and stimulation of guided tissue regeneration in the periodontal ligament [35]. The hPDLs used in this work were of a primary culture line and were supplied by the Escola Superior de Biotecnologia Universidade Católica in Porto, Portugal and bought from Innoprot (Spain).

4.1.2. Human Adipose Stem Cells (hASCs)

Human adipose-derived stem cells (hASCs) were chosen to be used in this thesis due to an increasing number of studies that were conducted using these cells for neurological-related therapies [37][46][67][69]. Those studies have verified that, when compared to other types of stem cells, hASCs can be easily isolated, have a high capacity of adhesion to materials and tissues and have also a high capability of differentiation [68]. Additionally, in those studies, the hASCs displayed high functional recovery rates, which further potentializes their use in tissue regeneration [67].

The hASCs used in this study came from a continuous culture line and were obtained from LaCell Inc (USA).

4.2. Cell culture method

The hASCs and hPDLs were cultured in α-MEM medium (Invitrogen, USA), with 10% Fetal Bovine Serum (FBS, Biochrom AG, Germany) and 1 % antibioticantimycotic solution – penicillin-streptomycin (Invitrogen, USA) and then stored at 37 °C and 5 % CO2 (v/v). The cultures were left to grow for about 72 hours while the produced CTR and MP membranes were cut with a puncture into small circular shaped samples of 1.00 cm diameter to fit within the wells of non-adherent 48-well plates (1.07 cm diameter). The samples were then sterilized with a 70% ethanol solution for 2 hours, after which the solution was removed, and the samples were washed three times with PBS and stored with a fourth pouring of PBS until the end of the cell growth period [7][25]. After the 72 hours, the cells were seeded in suspension in samples inside the wells and stored again at 37 ºC and 5 % CO2 (v/v) for 7 days until the ensuing studies were executed.

5. Cell viability

5.1. Cell quantification by immunostaining

Immunostaining is a technique that is commonly used to assess cell morphology, to detect a specific marker within a cell or cell culture, and to quantify the cell growth of a given culture. This method works by staining the target in the cell with a fluorescent dye that will allow for the observation on a microscope. The staining agent used for this was phalloidin (Sigma, USA), a bicyclic peptide that is known for being highly selective towards actin filaments present in eukaryotic cellular membranes. In addition, the fluorescent dye DAPI (4',6'-diamino-2-phenylindole) (Invitrogen, USA) was used conjugated with Phalloidin in order to guarantee entry to the cell and to taint the nucleus. This allowed for the observation of the cell distribution throughout the samples, their behaviour and to quantify the active cells [7][25].

Following cell culture and seeding of ASCs and PDLs on the MP and the CTR samples in wells, the cells were subjected to a 45 min period of fixation with 4 % paraformaldehyde (PFA, Panreac, Spain) at RT. Followingly, 0.3 % Triton X-100 was used for 10 min to permeabilize the cell membranes after which these were washed three times with PBS. Then, a PBS solution with 0.1 µg/ml phalloidin (Sigma, USA) and 1 µg/ml DAPI (Invitrogen, USA) was added to the cells for 45 min at RT. Next, the well plates with the samples were observed

using a confocal point-scanning microscope, Olympus FV 1000 (Olympus, USA), and three pictures were taken for counting the cells using ImageJ software (National Institutes of Health, USA). The pictures however came split into two: one picture in blue, for detecting nucleus with DAPI; and a same picture in red, to detect the cell structure with Pha. The pictures were then merged together via ImageJ software [7][25].

The results were expressed as the average of 4 measurements for each type of condition ± standard deviation.

5.2. Metabolic activity assay

This method consists of a colorimetric assay that allows for the determination of the viability or activity of a cell culture, via the use of a MTS solution (3-(4,5-dimethilthiazol-2-yl)-5-(3-carboxymethoxyphenyl)-2-(4-sulfophenyl)-2H-tetrazolium), which contains the dye tetrazolium. When the MTS is absorbed by the cells, tetrazolium is reduced by oxidoreductase enzymes dependent of NADPH into formazan, a brown or purple coloured compound. This only happens when the cell is viable, otherwise it will not reduce the tetrazolium dye.

The preparation of the samples for this assay required that a new culture medium was used due to the presence of a component in the α-MEM medium that disrupts the correct assessment of the absorbance by the samples. Accordingly, after the seeding of the cell cultures of ASCs and PDLs in the CTR and MP samples, the culture medium was removed, the samples were washed three times with PBS and a new medium DMEM:12, with of MTS in a 1:5 proportion, was added. This change of medium was made in dark conditions as the MTS is sensitive to the light and could, therefore, influence the reading of the absorbance. Next, the samples were taken in for a 3-hour incubation period after which they were taken to a NanoQuant infinite M200 (Tecan, Switzerland) spectrophotometer to have their absorbances read.

The results were expressed as the average of 4 measurements for each type of condition ± standard deviation.

6. Statistical analysis

The statistical analysis is a requirement when searching for the validation of any results in a study. For this thesis, the analysis was carried out on the IBM SPSS Statistics 24 software. Firstly, the conditions and variables where highlighted and organized, next the hypothesis of study were set, then the ideal statistical tests were identified and lastly the data was inputted on the software for the analysis.

The conditions in this study overall consisted on the two types of membranes produced, CTR and MP. However, depending on the practical tests, conditions like the state of hydration of the samples and the kind of cells seeded on each of the samples were also at play. The variables were relative to the results of each test, such as the results for the thickness measurement, CA, SFE, the mechanical properties, cell quantity and activity. As for the hypothesis at study, they focused on whether or not there were significant evidences to verify the differences between the conditions, so the null hypothesis (H_0) was always set to be the equality of the results, statistically, whilst the other hypothesis (H_1) stated the existence of difference between the results. Thus, in order to validate any of the hypothesis, the p-values (the probability of falsely denying the validity of the null hypothesis) had to be assessed in comparison to the confidence level of 95,00 %.

Upon the input of the results on the software, the normality of the data distribution for each method needed to be investigated firstly. For this evaluation, the test hypothesis was:

H_0: Data follows normal distribution

H_1: Data does not follow normal distribution

For every method performed in this study except for the CA measurement and SFE analysis, two factors were at play and being compared thus the statistical tests chosen were ANOVA One-Way and ANOVA Two-Way, followed by the Duncan *post-hoc* test. These types of test analyse the variances of data acquired, with one method comparing the groups of samples and using only one dependent variable whilst the second test uses more than one dependent variable. Additionally, the normality in these statistical tests is not required to be assessed. However, for the CA and SFE analysis there would only be one factor at play, so the normality of the data had to be verified firstly, using a t-student test for independent samples if the normality is observed. On the other hand, in the case the normality was not verified the data had to be transformed arithmetically with tools such as ln, log10, sqrt so that the distribution

would be normal and even if it was still not possible for that feature to be achieved, the statistical analysis had to be done with a non-parametric test. For these kinds of samples, the most adequate non-parametric test was Mann-Whitney, which is the equivalent to the t-student for independent samples.

IV. RESULTS AND DISCUSSION

1. Membranes' development

In this work, the membranes produced by solvent casting followed by a crystallization process that required an optimization step to induce water stabilization. As reported previously the crystallization of the membranes can be achieved using a water annealing process with an ethanol solution [31].

In the end, using this strategy, it was possible to obtain high quality membranes that were odourless and transparent. The MP membranes had micropatterned grooves that could be observed on a macroscopical scale, however the presence of the grooves created an opacity effect, as per seen in Figure 10.

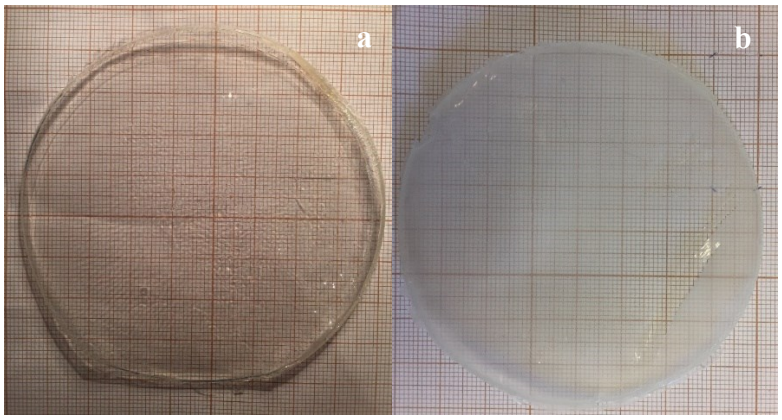

Figure 10. Representation of a CTR membrane (a) and a MP membrane (b).

On the other hand, the resulting CTR membranes showcased a smooth, homogenous and completely transparent surface. Those membranes were also highly malleable and resistant.

2. Morphological analysis by Scanning Electron Microscopy

The results of the SEM observation to one of the micropatterned membranes are presented in Figure 11. From the results, the topography of the grooves was analysed to greater detail, where the groves were seen to follow an almost straight pattern throughout the surface of the membrane. In the images, the grooves make up the darker lines, whereas the lighter areas are the plateaus.

Furthermore, the grooves displayed an average width of around 80 µm, whilst the plateaus averaged 130 µm of width. These results were satisfactory as, per previously stated, eukaryotic cells' average width varies from 10 to 100 µm, hence there is potential for the cells to fit in the grooves.

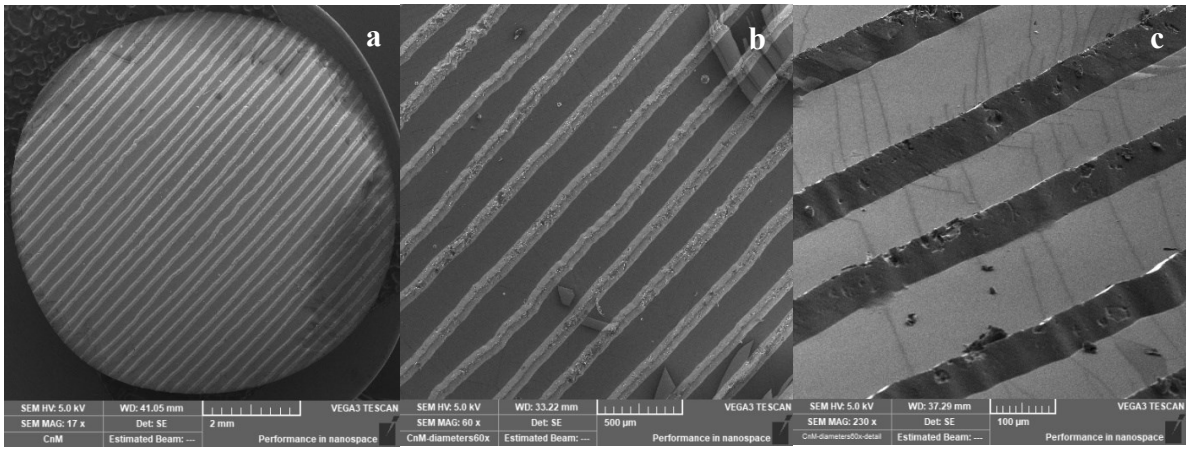

Figure 11. Image of the grooves in a MP membrane taken at 17 % (a), 60 % (b) and 230 % (c) magnification, adapted from SEM Vega-3-LM (TESCAN, USA).

3. Surface wettability and free energy by water contact angle

The results obtained from this characterization test are presented in Figure 12. The differences amongst the samples were validated statistically and considered to be significant ($p<0.01$ t-student test), hence the MP samples had higher CA than the CTR samples.

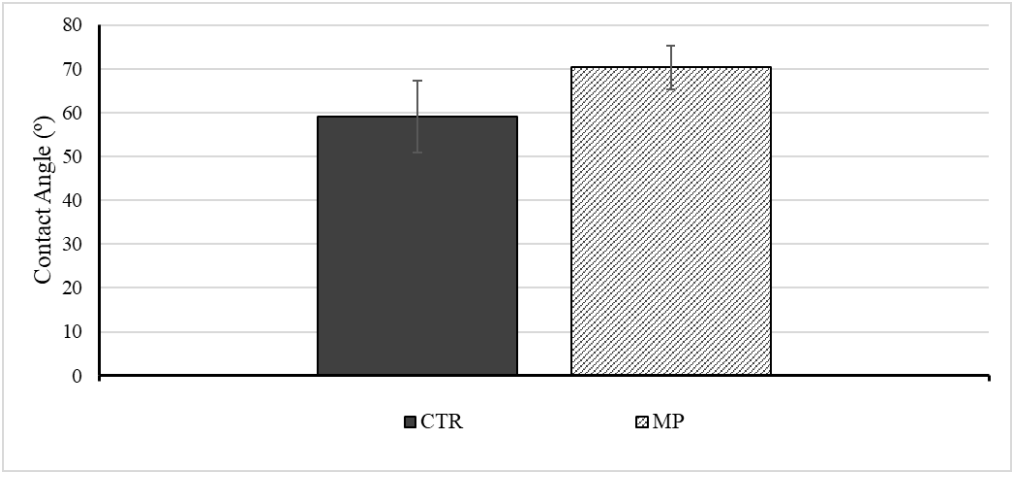

Figure 12. Comparison of the CA between CTR and MP samples.

Accordingly, the data of the CTR and MP samples was gathered resulting in average CAs of 59.05º ± 8.27 º and 70.31º ± 5.02. The difference in these results was validated statistically and the difference between the conditions was considered significant ($p<0.01$ t-student test), hence the MP had higher CA than the CTR.

Next, in order to calculate the SFE of the samples the CA was measured again using a second liquid with a dominant dispersive component, diiodomethane (MI). The results of the comparison can be observed in Figure 13.

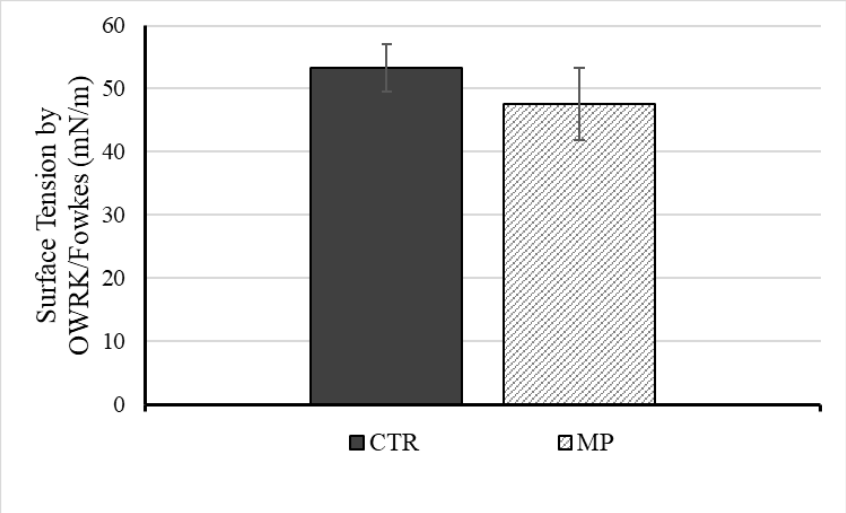

Figure 13. Comparison of the SFE between CTR and MP samples according to the OWRK/Fowkes method.

The SFE result of the CTR samples was 53.29 ± 3.70 mN/m whilst for the MP samples was 47.51 ± 5.71 mN/m. The difference between the samples was significant ($p=0.04$ t-student test) and in agreement with the Young equation, where a surface with high SFE has a tendency to be related to a lower CA whilst a low SFE is associated with a higher CA [8].

Both the contact angle and calculated surface energy have demonstrated that the micropattern have induced a higher hydrophobicity and, therefore, lower wettability of the MP samples. This can be explained according to the Cassie-Baxter effect which states that rough and heterogenous surfaces may still retain vapor under the drops used, thus creating a liquid-vapor interface between the surface and the drop [13]. The new interface then adds up to the

liquid-solid interface amongst the drop and the surface, as per schematized in Figure 14 [13][39].

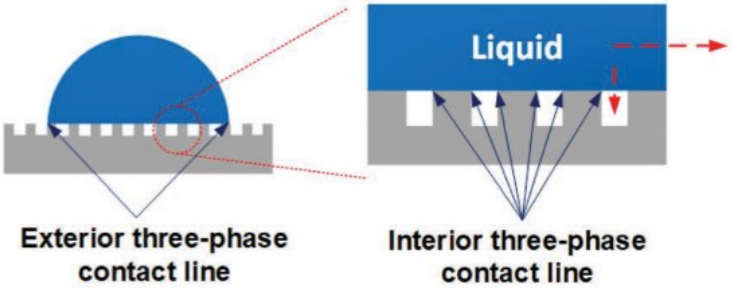

Figure 14. Schematic illustration of the three-phased interface acording to the Cassie-Baxter wetting effect. Adapted from [39].

The fact that the MP surface contains grooves makes it susceptible to retain air, which in contact with the drop forms a 180º contact angle and, given its positioning beneath the drop, makes up a repelling effect towards it, leading to a higher overall contact angle [52].

4. Thickness

The thickness of the membranes was measured prior to the mechanical testing due to its influence on the mechanical performance and because the setup of the testing required this parameter being known. The measurements were made in dry samples and in samples hydrated with PBS for 2 hours. The hydration was intended to reproduce the wet environment of living tissue where the membranes would, in theory, be applied.

The study of these measurements involved comparing the two types of samples and the two states of hydration (hydrated and non-hydrated). The results of the study are presented in Figure 15.

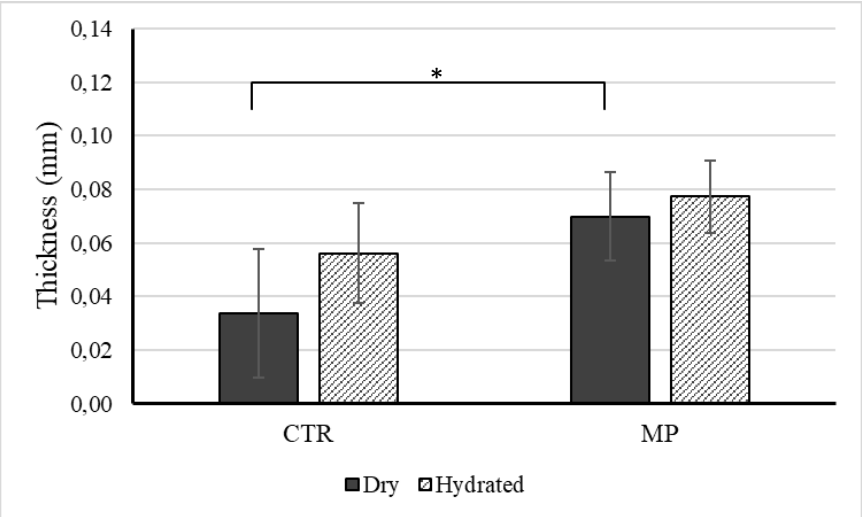

Figure 15. Comparison of the thickness between each CTR and MP samples, either dry or hydrated with PBS. (n=5, ANOVA One-Way, significant differences: *- p=0.03)

The results showed a higher thickness of the MP samples in comparison to the CTR samples, in dry and hydrated state. In fact, the CTR samples present a thickness of 0.03 ± 0.02 mm in the dry state and 0.06 ± 0.02 mm in the hydrated state while in the MP samples present a thickness of 0.07 ± 0.02 mm in the dry state and 0.08 ± 0.01 mm in the hydrated state. Also, the CTR samples showed a thickness increase (equation 11, appendix) of approximately 100 % whilst the MP samples only scored a 14.28 % increase. On first glance, this would be an indicator of how the hydration state influenced both types of membrane, with the most noticeable effect being on the CTR samples. However, the results from the comparison of the different hydration conditions amongst both CTR samples ($p=0.26$, ANOVA One-Way) and both MP samples ($p=0.91$, ANOVA One-Way), were not significant enough to be considered different. The results from the MP samples, in that regard, trace back to the surface wettability results and the Cassie-Baxter effect. In the case of the CTR samples however, water might have been absorbed to some extent, but not significantly to be statistically relevant.

On the other hand, the statistical analysis determined that the differences seen between the types of membrane were significant and valid ($p<0.01$, t-student test for independent samples). In fact, the differences observed between the dry CTR samples and dry MP samples have proven to be statistically significant ($p=0.03$, ANOVA One-Way). Therefore, the differences between the thickness of the samples were related to the type of membrane rather than their state of hydration.

5. Mechanical characterization

The study of the mechanical properties is one of upmost importance towards foreseeing the behavior of the membranes in a practical scenario. It allows for a clearer understanding of the ease which they can be handled and, moreover, their capacity to resist the stresses caused by physiological environment.

In the results of the Young's modulus, the CTR samples scored 0.40 ± 0.24 MPa in the dry state and 0.17 ± 0.08 MPa in the hydrated state, whilst the MP samples values were of 0.33 ± 0.09 MPa in the dry state and 0.09 ± 0.06 MPa in the hydrated state. The results of this mechanical property are shown in Figure 16.

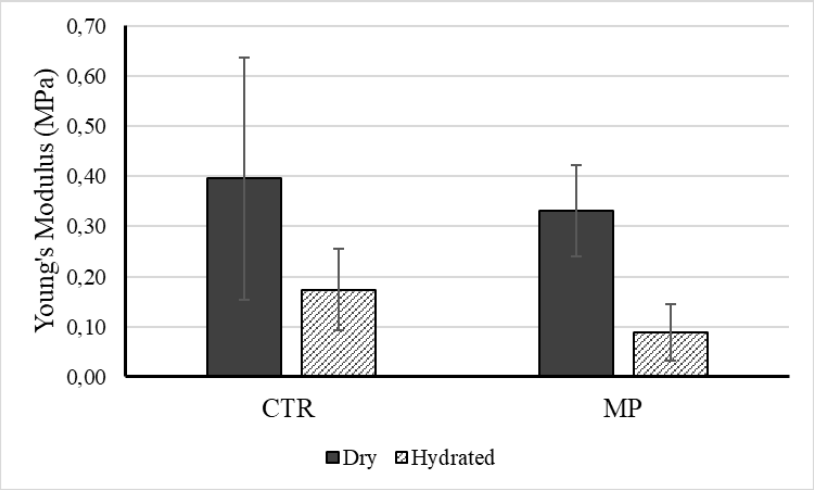

Figure 16. Results obtained for the Young's modulus of the different samples of membrane and hydration states.

Overall, the comparison between the states of hydration of all samples suggested that the dry samples had higher values than the hydrated samples. The result of that comparison was statistically significant ($p<0.01$ ANOVA Two-Way), meaning that the state of hydration was influential for the stiffness of the membranes, which was reflected by the lower values of the Young's modulus in the hydrated samples. These results suggest that when the water was absorbed into the amorphous zones of the polymer, it created a plasticizing effect on the samples [14]. A study made by Chang *et* al proposed a system where the water played a role as a dual plasticizer/anti-plasticizer in biopolymer films, via opposite entropic/free volume effects.

However, even though the CTR samples seemed to have overcome their respective MP counterparts, the statistics showed that there were not enough evidences (p=0.24 ANOVA Two-Way) to consider the type of membrane to be a factor towards their stiffness. Nevertheless, upon comparing both CTR samples and both MP samples as well as both dry samples (CTR and MP), no significant differences were found. Hence, the inconclusiveness of these results still remains unknown as to whether it is an outcome of the different hydration state, type of membrane or both these elements combined.

For the ultimate tensile strength (Figure 17), the CTR samples measured 4.70 ± 2.95 MPa in a dry state and 1.54 ± 0.48 MPa in a hydrated state. In the other hand, the MP samples scored 2.74 ± 0.78 MPa in a dry state and 1.03 ± 0.32 MPa in a hydrated state, which meant that by comparing each group of MP samples to the CTR samples in an identical state of hydration, the former exhibited lower values. Additionally, the same was observed as for the Young's modulus: results in the dry samples were higher than in the hydrated ones, and so too were they for the type of CTR membrane samples in comparison to the MP samples, overall.

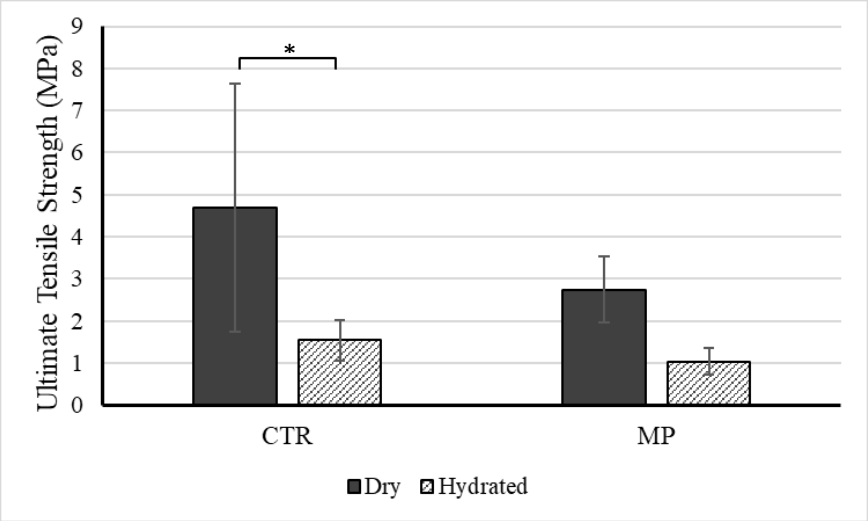

Figure 17. Results obtained of the ultimate tensile strength mechanical test to the different samples of membrane and hydration states. (n=5, ANOVA One-Way, significant differences: * -p=0.03)

In this mechanical property, yet again the results between the different hydration states, were different and significant, according to the statistical analysis (p<0.01 in an ANOVA Two-Way), although the results between the type of membranes were not enough to be considered different (p=0.10 ANOVA Two-Way). Upon comparing the different conditions of hydration

in each group of samples, differences were found amongst the CTR samples (p=0.03 ANOVA One-Way). These results suggest that the state of hydration was influential to the CTR samples, with the dry state granting more resistance to the membranes. However, the same was not observed amongst the MP samples (p=0.34, ANOVA One-Way), as the hydration state was not statistically enough influential to the outcomes. The type of membrane was also not influential, as the analysis between both CTR and MP dry samples was not significant (p=0.23, ANOVA One-Way).

The results of the elongation at break (Figure 18) followed a similar pattern as the results in the previous mechanical properties with the dry samples demonstrating more elongation at the point of break than the hydrated samples. The CTR dry samples achieved 48.56 ± 28.41 % of elongation and only 21.77 ± 6.58 % in the hydrated samples, whereas the MP samples reached 25.17 ± 12.90 % of elongation in dry samples and 14.14 ± 4.33 % in the hydrated ones.

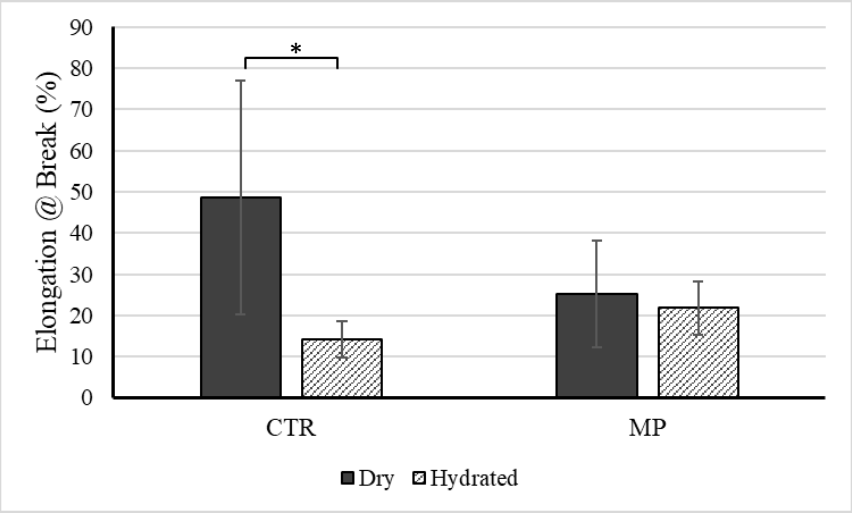

Figure 18. Results obtained of the elongation at break mechanical test to the different samples of membrane and hydration states. (n=5, ANOVA One-Way, significant differences: * -p=0.02)

In this property, the behavior was different between the hydrated samples, as the MP samples scored higher elongation rates than the CTR samples. Yet, although this behavior was not seen in the other properties, such difference had no statistical value and therefore it might have been an outlying result. In fact, the results of this property were analyzed, and the statistics showed that the differences in terms of the hydration state were significant (p=0.02 ANOVA Two-Way) although the same could not be stated for the differences between the membrane

types (p=0.29 ANOVA Two-Way). However, upon further analysis, the state of hydration proved to be statistically influential only on the CTR samples (p=0.02 ANOVA One-Way) as the MP samples showed no significant results (p=0.99, ANOVA One-Way). Also, no differences were found between both CTR and MP dry samples (p=0.14, ANOVA One-Way), hence reinforcing the fact that the type of membrane was not influential to this mechanical property either.

The explanation for the results obtained in the mechanical tests can be related to reports from other studies which conclude that water increases mobility in the membranes, as it frequently creates bonds with Gly [11][51]. Although, upon the conformational shift of the SF towards a β-sheet formation, there are ruptures to the hydrogen bonds that leave the hydrogen bonding sites exposed for interaction with water molecules from the aqueous media, thus becoming highly reactive. This has been reported to cause a decrease in the brittleness of silk based materials [11]. Additionally, Minoura et al. have also reported that the presence of water increases the softness of the silk membranes, thus supporting the behavior of water as creating a plasticizer effect [53].

However, the same was not found in this study, as the hydrated membranes displayed more brittleness then the dry membranes. In fact, regardless of the type of membranes used, the dry samples presented more elasticity and resistance. The explanation to these results can revert to the crystallization technique used in this work as it has been reported that when treating β-pleated sheets of fibroin peptides with solvents such as methanol and ethanol, materials become insoluble in water yet brittle and rigid when dry [31]. For that reason, different plasticizers such as Gly are used to reduce the rigidity of the dry materials by promoting structural changes which result in increased crystallinity, softness and flexibility [11].

In this work, glycerol was indeed added to the SF solution and the crystallization was done by a water annealing treatment with a 70% ethanol solution, thus explaining the softness, flexibility and resistance of the dry membranes. Nevertheless, in the hydrated samples, the aqueous solution of PBS might have been responsible for promoting the removal of the glycerol, hence these samples became more brittle and rigid than the dry samples. Moreover, the end results showed that the mechanical performances of the MP and the CTR membranes could not be deemed as different enough between each other, thus meaning that it is possible to produce membranes with defined micropatterned surfaces maintain the same structural and physical attributes.

6. Cell adhesion and proliferation

The immunostaining assay with Pha/DAPI served two purposes, the first of which being the quantification of cells per samples and the second objective was to observe how the cells behaved and spread throughout the sample. Figures 19 and 20 show some of the obtained images from the immunostaining to the samples with hASCs and hPDLs, respectively. Figure 21 shows the average number of cells per sample.

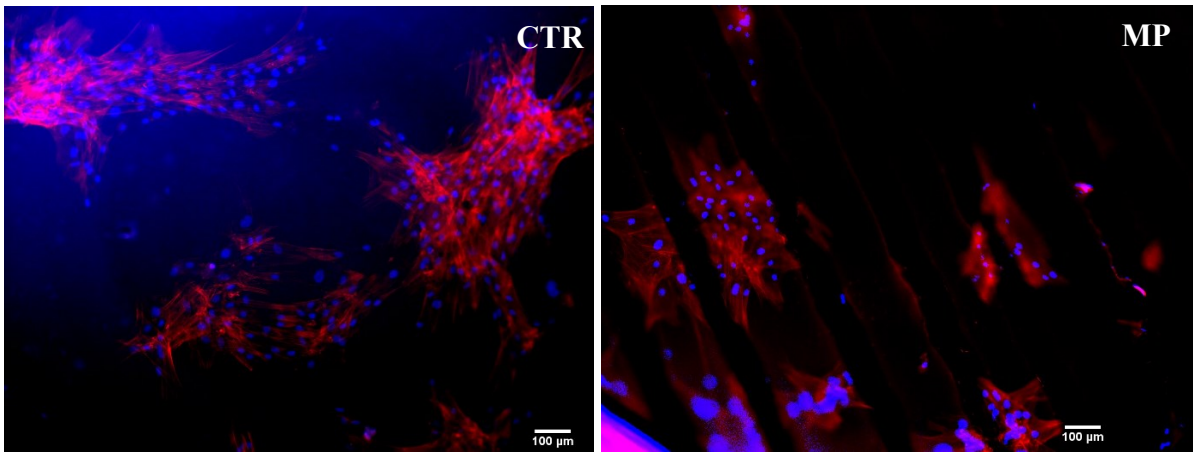

Figure 19. Cellular morphology of the CTR and MP hASC samples. Pictures taken at 10x magnification using confocal point-scanning microscope, Olympus FV 1000 (Olympus, USA), and treated with ImageJ software (National Institutes of Health, USA).

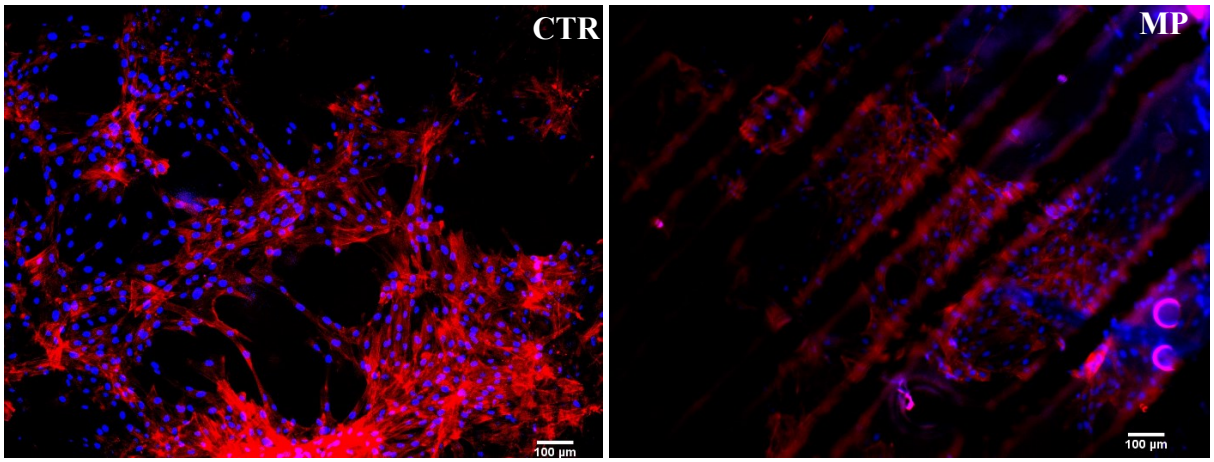

Figure 20. Cellular morphology of the CTR and MP hPDL samples. Pictures taken at 10x magnification using confocal point-scanning microscope, Olympus FV 1000 (Olympus, USA), and treated with ImageJ software (National Institutes of Health, USA).

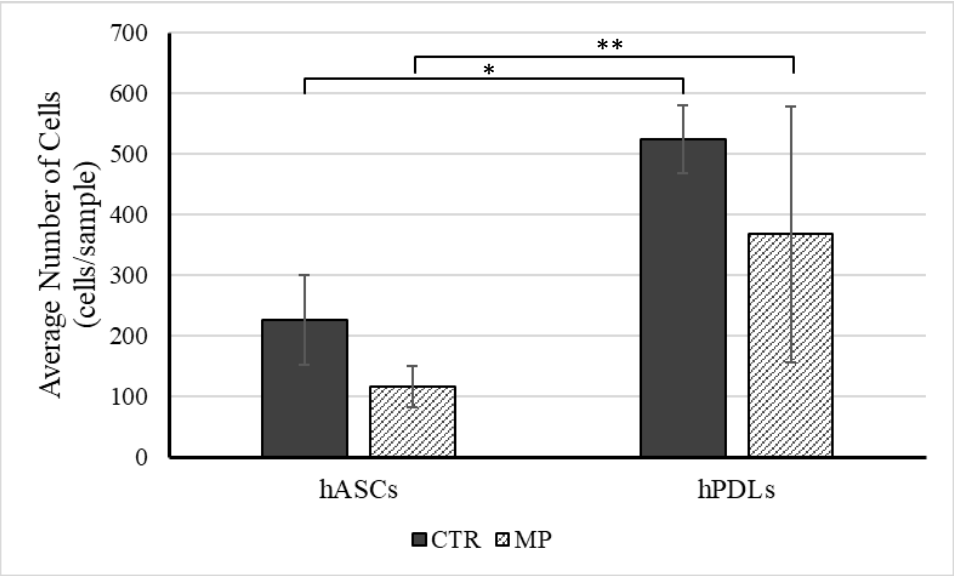

Figure 21. Average hASCs and hPDLs count in CTR and MP samples. (n=4, ANOVA One-Way, significant differences: * - $p<0.01$; ** - $p<0.01$)

In this study, both types of cell adhered and created clusters throughout the samples even though they failed to grow out according to the patterns of the MP samples. Since one of the interests of this work was to promote the cell proliferation and distribution according to the patterning of the surface, the results of this observation were very anticipated. However, it was not possible to observe this behaviour from the cells. In fact, the SEM analysis results may help justify this behaviour from the cells, as the plateau zones observed proved to be much wider in comparison to the grooves. This allowed the freedom for the cells to grow randomly throughout the surface of the membrane. Nevertheless, the cells used the grooves of the patterning instead for bridging over, transversally, on to the next plateau zone. This reflects that even though the cells did not use the grooves to position themselves accordingly, they may assume a different kind of patterning by positioning themselves across the patterns, instead. In fact, this kind of behaviour has been previously reported by Baran et al, with mouse fibroblasts [9].

As for the differences in the adhesion between cells, not only did the hPDLs adhere more to the samples but the cells overall adhered more onto the CTR samples rather than the MP samples. In fact, the average number of cells accounted for in CTR samples was 226.08 ± 73.64 hASCs and 523.75 ± 56.18 hPDLs whilst in MP samples they averaged 116.67 ± 34.03 hASCs and 367.50 ± 211.01 hPDLs. These results were approved statistically, as the number of cells accounted for in between both kinds of membrane samples (CTR or MP) ($p=0.01$ ANOVA Two-Way) and cell types ($p<0.01$ ANOVA Two-Way) were significant. Moreover,

the comparison between all groups of samples reiterated those outcomes, as differences were found amongst both CTR groups ($p<0.01$ ANOVA One-Way) and both MP groups ($p<0.01$ ANOVA One-Way). Nonetheless, the comparison between both hASCs samples ($p=0.29$, ANOVA One-Way) and between both hPDLs samples ($p=0.08$, ANOVA One-Way) showed that there were no significant differences between the type of membrane used in each cell type.

These results, however significantly different from each other, reflect that not only do the hPDLs show better adhesion potential but also show that the types of membranes used were not influential for the outcomes of this assay. In hindsight, other results from this work, namely the CA of the samples, would suggest that the presence of micropatterns and the Cassie-Baxter effect, caused by their presence, would hinder the cell adhesion onto the MP samples. However, as such as was not completely the case, the Cassie-Baxter effect constitute a cause for there not have been such noticeable cell adhesion in the grooves.

7. Metabolic activity assay

This colorimetric assay looked to assess the viability of the cells that adhered to the samples. This achievement was accomplished by measuring the absorbance of the cells in the samples at 490 nm, with a spectrophotometer. Here, the criteria were that if the cells were viable, they would have reduced the MTS into formazan (coloured purple or brown), which bears a different colour than the MTS. This change of colour was then measured, and the results were printed. Figure 22 shows the well plate after the addition of MTS to the samples and Figure 23 displays the results of the absorbances read for the samples of different membrane types, with different cell types.

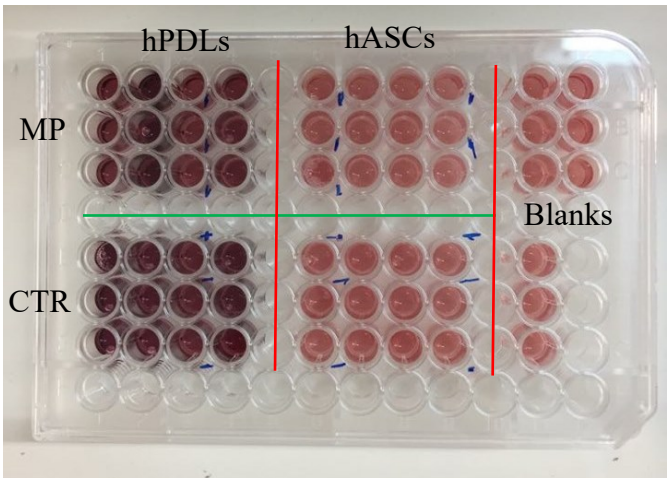

Figure 22. 48-Well plate with samples after the addition of MTS. The dark coloured wells are the samples with hPDLs, whilst the lighter coloured wells are the samples with hASCs. The nine wells on the right side of the plate are the blanks that were used to subtract the absorbance of the membranes from the other samples.

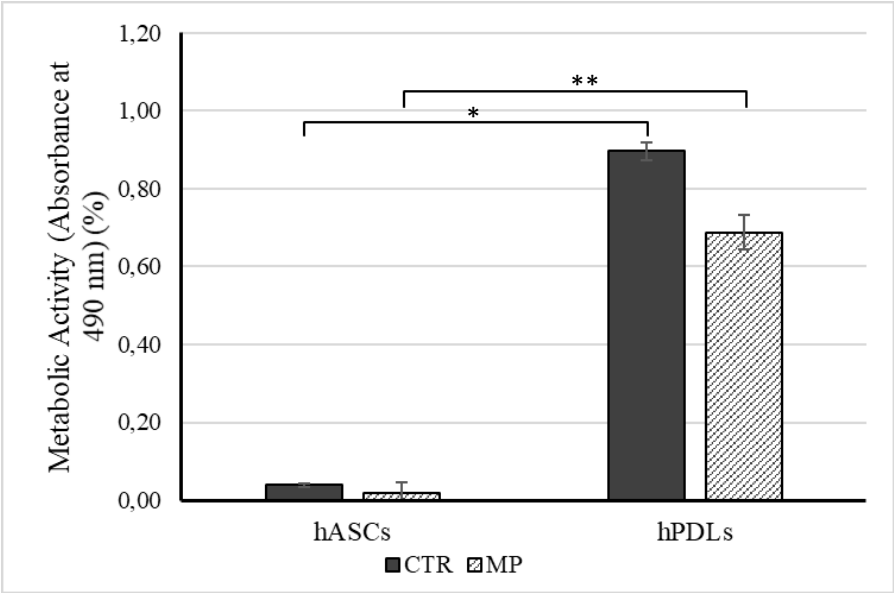

Figure 23. Results of the absorbances read for the CTR and MP samples, with different cell types (hASCs and hPDLs), at 490 nm. (n=4, ANOVA One-Way, significant differences: * - $p<0.01$; ** -$p<0.01$)

Upon first look at Figure 22, it is possible to observe that the colour differences between the samples with different cell types are significant, this foreshadowed that there had been more adhesion of hPDLs to the membranes and that the viability was also higher in the samples with those cells. On the other hand, it is difficult to perceive any difference in the results when the types of membranes are considered.

In Figure 23, however, the results were seemingly very close between either type of membrane samples and also very similar to the results of the cell adhesion assay, overall. Effectively, the metabolic activity measured in the CTR samples was of 0.04 ± 0.00 with hACSs and 0.90 ± 0.02 with hPDLs, whereas the MP samples measured 0.02 ± 0.02 with hASCs and 0.69 ± 0.04 with hPDLs. After the statistical analysis was made, the results showed that the differences between the different cell types was in fact significant ($p<0.01$ ANOVA Two-Way) though the same could not be stated about the different types of membrane used ($p=0.23$ ANOVA Two-Way). Furthermore, analysis between all sample groups suggested that the differences within both CTR samples ($p<0.01$ ANOVA One-Way) and both MP samples ($p<0.01$ ANOVA One-Way) were significant. However, alike the cell adhesion results, the statistical analysis to the results of both hASCs samples ($p=1.00$, ANOVA One-Way) and between both hPDLs samples ($p=0.40$, ANOVA One-Way) proved that no significant differences exist between the type of membrane used in each cell type. This meant that not only did the hPDLs cells displayed more metabolic activity but also that the metabolic activity was not influenced by the type of membrane used. The results from this assay go hand to hand with the results from the previous assay for cell adhesion, as expected.

V. CONCLUSIONS

In this study, it was possible to successfully develop SF membranes with micropatterned surfaces. Thus, the ability of the SF solution to be cast, adapt and assume the topography of a given mould was verified and confirmed. The observation was done both macroscopically in the naked eye and also via SEM scanning.

Followingly, the wettability of the membranes, analysed by measuring their CA and SFE, offered interesting insight towards their interfacial behaviour with liquid and aqueous solutions. Those interfacial interactions reflected the influence caused by the changes in the materials with the introduction of patterns and also allowed for an understanding of the potential for cell growth and cell behaviour in the membranes. In fact, despite the patterns having had a repelling factor towards liquids, hence potentially hindering cell adhesion, such was accomplished, nonetheless. Consequently, the cell viability was ensured, according to the cell assays where adhesion and metabolic activity were recorded in both kinds of cells and in both types of membranes used. The results of these assays showed that better adhesion and activity was achieved with hPDLs and that the type of membrane used was not influential for cell viability.

Additionally, the results obtained for the mechanical properties reflected that, even though the same amount of solution volume was used to produce the membranes, their conformation (as a result of the different moulding areas) caused differences to their thickness, with the MP samples being presented as thicker. However, this did not influence or change their mechanical performance as the type of membrane used was not influential to the samples' mechanical performance but rather their state of hydration. In fact, the results of the mechanical tests, although lower than the results achieved in other studies, were proportional to those studies, as their different production methods should be taken into consideration [19][23]. Furthermore, the membranes produced were flexible, malleable and resistant, making them apt for further use in research for guided tissue regeneration and for the application of these membranes in either external drier areas or in internal and wet areas.

Other studies with SF membranes and their characterization, tested other physicochemical and biochemical properties typical of this material [19][23]. These studies observed the antioxidant activity of these membranes as well as their degradability rates, which are both interesting qualities for the desired application of the membranes in this study. As mentioned previously, injuries and wounds often come associated with toxic and reactive agents

that inhibit the regeneration and healing of the damaged tissue, hence the antioxidant nature of this material allows for a dispersion of these agents. Additionally, it is important for the membranes to remain intact long enough for the cells to form biofilms and fully repair the damaged areas of biological tissue and then suffer degradation once their purpose is achieved. Therefore, these characteristics of SF membranes, accoupled with micropatterns, make up for very interesting and promising products for tissue engineering and the health markets.

VI. FUTURE WORKS

The area of tissue engineering allows for a wide variety of extensive researches set for a better understanding of the behaviour and relationship between biology and materials science, whose main benefactor can only be life itself. Guided tissue regeneration, as a part of tissue engineering technologies has been demonstrating an ever more significant potential for the treatment of injuries and disease-caused damages to biological tissues. However, some work remains yet to be done and some obstacles to be overcome.

In relation to this work, a few aspects would benefit from some of that progress. For instance, the printing of patterns in a surface and the production of moulds should be perfected, not only for the betterment of the quality of the patterning but also for the availability of different types of patterns. On this matter, new types of moulds should be researched and developed to allow for different means of crystallization of the MP membranes to take place. Furthermore, studies should be conducted as for how the presence of patterns affects both the antioxidant activity and the degradability rates of the membranes. Additionally, for the cell culture, other cells should be tested in these types of material with the possibility to add growth factors such as proteins, gels or other compounds to promote cell adhesion and growth throughout the surface of the material and according to the patterns, as that was not possible to be exercised in this thesis. These membranes could also benefit from *in vivo* testing and the adding of antibiotics or other drugs in order to respond to toxic and reactive agents, which are typical of damaged tissue and injuries.

REFERENCES

[1] About vinyl. (2017). Retrieved from http://www.gzvinyl.com/About-vinyl.aspx

[2] Abu-Rub, M., McMahon, S., Zeugolis, D. I., Windebank, A., & Pandit, A. (2010). Spinal cord injury in vitro: Modelling axon growth inhibition. *Drug Discovery Today*, *15*(11–12), 436–443. https://doi.org/10.1016/j.drudis.2010.03.008

[3] Aljehani, Y. A. (2014). *Risk Factors of Periodontal Disease : Review of the Literature*. *2014*.

[4] Alom Ruiz, S., & Chen, C. S. (2007). Microcontact printing: A tool to pattern. *Soft Matter*, *3*(2), 168–177. https://doi.org/10.1039/b613349e

[5] Altman, G. H., Diaz, F., Jakuba, C., Calabro, T., Horan, R. L., Chen, J., … Kaplan, D. L. (2003). Silk-based biomaterials. *Biomaterials*, (24), 401–416. https://doi.org/10.1016/j.bone.2006.04.019

[6] Arx, T. Von, & Berne, C.-. (n.d.). *Horizontal ridge augmentation using autogenous block grafts and the guided bone regeneration technique with collagen membranes : a clinical study with 42 patients*. 359–366. https://doi.org/10.1111/j.1600-0501.2005.01234.x

[7] Assunção-Silva, R. C., Oliveira, C. C., Ziv-Polat, O., Gomes, E. D., Sahar, A., Sousa, N., … Salgado, A. J. (2015). Induction of neurite outgrowth in 3D hydrogel-based environments. *Biomedical Materials (Bristol)*, *10*(5). https://doi.org/10.1088/1748-6041/10/5/051001

[8] Attension, technical note. (2013). Surface free energy - theory and calculations. *Lecture on Contact Angles*, *3*(1), 457–460. https://doi.org/10.1073/pnas.1201800109

[9] Baran, E. T., Salgado, A., & Reis, R. L. (2004). *Multichannel mould processing of 3D structures from microporous coralline hydroxyapatite granules and chitosan support materials for guided tissue regeneration / engineering*. (March 2004). https://doi.org/10.1023/B

[10] Berthiaume, F., Maguire, T. J., & Yarmush, M. L. (2011). Tissue Engineering and Regenerative Medicine: History, Progress, and Challenges. *Annual Review of Chemical and Biomolecular Engineering*, *2*(1), 403–430. https://doi.org/10.1146/annurev-chembioeng-061010-114257

[11] Brown, J. E., Davidowski, S. K., Xu, D., Cebe, P., Onofrei, D., Holland, G. P., & Kaplan, D. L. (2016). Thermal and Structural Properties of Silk Biomaterials Plasticized by Glycerol. *Biomacromolecules*, *17*(12), 3911–3921.

https://doi.org/10.1021/acs.biomac.6b01260

[12] Carvalho, A., Pelaez-Vargas, A., Gallego-Perez, D., Grenho, L., Fernandes, M. H., De Aza, A. H., … Monteiro, F. J. (2012). Micropatterned silica thin films with nanohydroxyapatite micro-aggregates for guided tissue regeneration. *Dental Materials*, *28*(12), 1250–1260. https://doi.org/10.1016/j.dental.2012.09.002

[13] Cassie, A. B. D. (1948). Contact Angels. *Discuss. Faraday Soc.*, *3*, 11–16.

[14] Chang, Y. P., Cheah, P. B., & Seow, C. C. (2000). Plasticizing – Antiplasticizing Effects of Water on Physical Properties of Tapioca. *Journal of Food Science*, *65*(3).

[15] Chen, S., Nakamoto, T., Kawazoe, N., & Chen, G. (2015). Biomaterials Engineering multi-layered skeletal muscle tissue by using 3D microgrooved collagen scaffolds. *Biomaterials*, *73*, 23–31. https://doi.org/10.1016/j.biomaterials.2015.09.010

[16] D'Arcangelo, E., & McGuigan, A. P. (2015). Micropatterning strategies to engineer controlled cell and tissue architecture in vitro. *BioTechniques*, (58), 13–23. https://doi.org/10.2144/000114245

[17] Falconnet, D., Csucs, G., Michelle Grandin, H., & Textor, M. (2006). Surface engineering approaches to micropattern surfaces for cell-based assays. *Biomaterials*, *27*(16), 3044–3063. https://doi.org/10.1016/j.biomaterials.2005.12.024

[18] Farkas, G. J., Gorgey, A. S., Dolbow, D. R., Berg, A. S., David, R., Farkas, G. J., … Gater, D. R. (2017). profiles The influence of level of spinal cord injury on adipose tissue and its relationship to inflammatory adipokines and cardiometabolic profiles. *The Journal of Spinal Cord Medicine*, *0*(0), 1–9. https://doi.org/10.1080/10790268.2017.1357918

[19] Fernandes, A. (2019). *Biofunctional silk-fibroin membranes with antioxidant properties for the treatment of chronic wounds*.

[20] Francis Suh, J. K., & Matthew, H. W. T. (2000). Application of chitosan-based polysaccharide biomaterials in cartilage tissue engineering: A review. *Biomaterials*, *21*(24), 2589–2598. https://doi.org/10.1016/S0142-9612(00)00126-5

[21] Fujihara, K., Kotaki, M., & Ramakrishna, S. (2005). *Guided bone regeneration membrane made of polycaprolactone / calcium carbonate composite nano-fibers*. *26*, 4139–4147. https://doi.org/10.1016/j.biomaterials.2004.09.014

[22] Gao, M., Lu, P., Bednark, B., Lynam, D., Conner, J. M., Sakamoto, J., & Tuszynski, M. H. (2013). Biomaterials Templated agarose scaffolds for the support of motor axon regeneration into sites of complete spinal cord transection. *Biomaterials*, *34*(5), 1529–1536. https://doi.org/10.1016/j.biomaterials.2012.10.070

[23] Geão, C. B. (2017). *Development of new bombyx mori silk fibroin membranes for periodontal guided tissue regeneration*.

[24] Gerberich, B. G., & Bhatia, S. K. (2013). Tissue scaffold surface patterning for clinical applications. *Biotechnology Journal*, *8*(1), 73–84. https://doi.org/10.1002/biot.201200131

[25] Gomes, E. D., Mendes, S. S., Leite-Almeida, H., Gimble, J. M., Tam, R. Y., Shoichet, M. S., … Salgado, A. J. (2016). Combination of a peptide-modified gellan gum hydrogel with cell therapy in a lumbar spinal cord injury animal model. *Biomaterials*, *105*, 38–51. https://doi.org/10.1016/j.biomaterials.2016.07.019

[26] Guillot, P. V., Cui, W., Fisk, N. M., & Polak, D. J. (2007). Stem cell differentiation and expansion for clinical applications of tissue engineering: Tissue Engineering Review Series. *Journal of Cellular and Molecular Medicine*, *11*(5), 935–944. https://doi.org/10.1111/j.1582-4934.2007.00106.x

[27] Hacking, S. A., & Khademhosseini, A. (2009). *Applications of Microscale Technologies for Regenerative Dentistry*. https://doi.org/10.1177/0022034509334774

[28] Hessberger, R. W. (2017). Stages of Gum Disease & Periodontal Treatment – Chicago, IL. Retrieved from https://www.dentistnorthwestchicago.com/blog/2017/12/23/stages-of-gum-disease-188171

[29] Hoffman, T., Khademhosseini, A., & Langer, R. (2019). Chasing the Paradigm: Clinical Translation of 25 Years of Tissue Engineering. *Tissue Engineering Part A*, *25*(9–10), 679–687. https://doi.org/10.1089/ten.tea.2019.0032

[30] Hofmann, S., Po, C. T. W., Rossetti, F., Textor, M., & Vunjak-novakovic, G. (2006). *Silk fibroin as an organic polymer for controlled drug delivery*. *111*, 219–227. https://doi.org/10.1016/j.jconrel.2005.12.009

[31] Hu, X., Shmelev, K., Sun, L., Gil, E., Park, S., Cebe, P., & Kaplan, D. L. (2011). *Regulation of Silk Material Structure by Temperature-Controlled Water Vapor Annealing*. 1686–1696.

[32] Hughes, M. P. (2002). *Review Strategies for dielectrophoretic separation in laboratory-on-a-chip systems*. 2569–2582.

[33] Imamura, Y., Mukohara, T., Shimono, Y., & Funakoshi, Y. (2015). *Comparison of 2D- and 3D-culture models as drug-testing platforms in breast cancer*. 1837–1843. https://doi.org/10.3892/or.2015.3767

[34] Ito, Y. (1999). *Surface micropatterning to regulate cell functions*. *20*.

[35] Jönsson, D., Nebel, D., Bratthall, G., & Nilsson, B. O. (2011). The human periodontal

ligament cell: A fibroblast-like cell acting as an immune cell. *Journal of Periodontal Research*, *46*(2), 153–157. https://doi.org/10.1111/j.1600-0765.2010.01331.x

[36] Kai, D., Prabhakaran, M. P., Jin, G., & Ramakrishna, S. (2011). *Polypyrrole-contained electrospun conductive nanofibrous membranes for cardiac tissue engineering*. 376–385. https://doi.org/10.1002/jbm.a.33200

[37] Kang, S., Shin, M., Jung, J. I. N. S. U. P., & Kim, Y. G. (2006). *Autologous Adipose Tissue-derived Stromal Cells for Treatment of Spinal Cord Injury*. *594*, 583–594.

[38] Kowalczewski, C. J., & Saul, J. M. (2018). Biomaterials for the delivery of growth factors and other therapeutic agents in tissue engineering approaches to bone regeneration. *Frontiers in Pharmacology*, *9*(MAY), 1–15. https://doi.org/10.3389/fphar.2018.00513

[39] Kung, C. H., Sow, P. K., Zahiri, B., & Mérida, W. (2019). *Assessment and Interpretation of Surface Wettability Based on Sessile Droplet Contact Angle Measurement : Challenges and Opportunities*. *1900839*, 1–27. https://doi.org/10.1002/admi.201900839

[40] Kvist, M., Sondell, M., Kanje, M., & Dahlin, L. B. (2011). *Regeneration in , and properties of , extracted peripheral nerve allografts and xenografts*. *1*(February), 122–128. https://doi.org/10.3109/2000656X.2011.571847

[41] Lee, K., Silva, E. A., & Mooney, D. J. (2011). Growth factor delivery-based tissue engineering: General approaches and a review of recent developments. *Journal of the Royal Society Interface*, *8*(55), 153–170. https://doi.org/10.1098/rsif.2010.0223

[42] Liao, S., Wang, W., Uo, M., Ohkawa, S., Akasaka, T., Tamura, K., … Watari, F. (2005). *A three-layered nano-carbonated hydroxyapatite / collagen / PLGA composite membrane for guided tissue regeneration*. *26*, 7564–7571. https://doi.org/10.1016/j.biomaterials.2005.05.050

[43] Linde, A., Alberius, P., & Dahlin, C. (n.d.). *Osteopromotion : A Soft-Tissue Exclusion Principle Using a Membrane for Bone Healing and Bone Neogenesis **. 1116–1128.

[44] Liu, S., Xie, Y., & Wang, B. (2018). *Role and prospects of regenerative biomaterials in the repair of spinal cord injury*. https://doi.org/10.4103/1673-5374.253512

[45] Luz, G. M., Boesel, L., & Mano, F. (2012). *Micropatterning of Bioactive Glass Nanoparticles on Chitosan Membranes for Spatial Controlled Biomineralization*.

[46] Ma, Z., Lu, Y., Yang, Y., Wang, J., & Kang, X. (2019). *Research progress and prospects of tissue engineering scaffolds for spinal cord injury repair and protection*. (Figure 1).

[47] Mann, E. E., Manna, D., Mettetal, M. R., May, R. M., Dannemiller, E. M., Chung, K. K., … Reddy, S. T. (2014). Surface micropattern limits bacterial contamination. *Antimicrobial Resistance and Infection Control*, *3*(1). https://doi.org/10.1186/2047-2994-3-28

[48] Marina, A., Gentile, P., Chiono, V., & Ciardelli, G. (2012). Acta Biomaterialia Collagen for bone tissue regeneration. *Acta Biomaterialia*, *8*(9), 3191–3200. https://doi.org/10.1016/j.actbio.2012.06.014

[49] Martinez-Rivas, A., González-Quijano, G. K., Proa-Coronado, S., Séverac, C., & Dague, E. (2017). Methods of micropatterning and manipulation of cells for biomedical applications. *Micromachines*, *8*(12). https://doi.org/10.3390/mi8120347

[50] Mata, A., Boehm, C., Fleischman, A. J., Muschler, G., Roy, S., & Al, M. E. T. (2002). *Growth of connective tissue progenitor cells on microtextured polydimethylsiloxane surfaces*.

[51] Meyers, M. A., Chen, P. Y., Lin, A. Y. M., & Seki, Y. (2008). Biological materials: Structure and mechanical properties. *Progress in Materials Science*, *53*(1), 1–206. https://doi.org/10.1016/j.pmatsci.2007.05.002

[52] Milne, A. J. B., & Amirfazli, A. (2012). The Cassie equation: How it is meant to be used. *Advances in Colloid and Interface Science*, *170*(1–2), 48–55. https://doi.org/10.1016/j.cis.2011.12.001

[53] Minoura, N., Tsukada, M., & Nagura, M. (1990). Physico-chemical properties of silk fibroin membrane as a biomaterial. *Biomaterials*, *11*(6), 430–434. https://doi.org/10.1016/0142-9612(90)90100-5

[54] Nagpal, R., Yamashiro, Y., & Izumi, Y. (2015). *The Two-Way Association of Periodontal Infection with Systemic Disorders : An Overview*. *2015*.

[55] Naseer, S. M., Manbachi, A., Samandari, M., Walch, P., Gao, Y., Zhang, Y. S., … Shin, S. R. (2017). Surface acoustic waves induced micropatterning of cells in gelatin methacryloyl (GelMA) hydrogels. *Biofabrication*, *9*(1), 015020. https://doi.org/10.1088/1758-5090/aa585e

[56] Nazir, M. A. (2017). *Prevalence of periodontal disease , its association with systemic diseases and prevention*. *1*(2).

[57] Panawala, L. (2017). *Difference Between Prokaryotic and Eukaryotic Cells Main Difference – Prokaryotic vs Eukaryotic Cells*. (February).

[58] Parker, J. A. T. C., Walboomers, X. F., Hoff, J. W. V. Den, Maltha, J. C., Jansen, J. A., & Al, P. E. T. (2001). *Soft-tissue response to silicone and poly- L -lactic acid implants*

with a periodic or random surface micropattern. 13–17.

[59] Petite, H., Viateau, V., Bensaïd, W., Meunier, A., Pollak, C. De, Bourguignon, M., … Guillemin, G. (2000). *Nbt0900_959*. 1–5.

[60] Pilipchuk, S. P., Fretwurst, T., Yu, N., Larsson, L., Kavanagh, N. M., Asa'ad, F., … Giannobile, W. V. (2018). Micropatterned Scaffolds with Immobilized Growth Factor Genes Regenerate Bone and Periodontal Ligament-Like Tissues. *Advanced Healthcare Materials*, *7*(22), 1–11. https://doi.org/10.1002/adhm.201800750

[61] Pilipchuk, S. P., Monje, A., Jiao, Y., Hao, J., Kruger, L., Flanagan, C. L., … Giannobile, W. V. (2016). *Integration of 3D Printed and Micropatterned Polycaprolac- tone Scaffolds for Guidance of Oriented Collagenous Tissue Formation In Vivo*. 676–687. https://doi.org/10.1002/adhm.201500758

[62] Quist, A. P., & Oscarsson, S. (2010). Micropatterned surfaces: techniques and applications in cell biology. *Expert Opinion on Drug Discovery*, *5*(6), 569–581. https://doi.org/10.1517/17460441.2010.489606

[63] Recknor, J. B., Sakaguchi, D. S., & Mallapragada, S. K. (2006). *Directed growth and selective differentiation of neural progenitor cells on micropatterned polymer substrates*. *27*, 4098–4108. https://doi.org/10.1016/j.biomaterials.2006.03.029

[64] Riboldi, S. A., Sampaolesi, M., Neuenschwander, P., Cossu, G., & Mantero, S. (2005). *Electrospun degradable polyesterurethane membranes : potential scaffolds for skeletal muscle tissue engineering*. *26*, 4606–4615. https://doi.org/10.1016/j.biomaterials.2004.11.035

[65] Rossi, M., & Pagliaro, M. (2008). Glycerol: Properties and Production. *Future of Glycerol: New Usages for a Versatile Raw Material*, 1–17.

[66] Ryan, B. J., & Poduska, K. M. (2014). *Roughness effects on contact angle measurements Roughness effects on contact angle measurements*. *1074*(2008). https://doi.org/10.1119/1.2952446

[67] Ryu, H., Lim, J., Byeon, Y., Park, J., Seo, M., Lee, Y., & Hee, W. (2009). *Veterinary Science Functional recovery and neural differentiation after transplantation of allogenic adipose-derived stem cells in a canine model of acute spinal cord injury*. *10*, 273–284. https://doi.org/10.4142/jvs.2009.10.4.273

[68] Salgado, A. J. B. O. G., Reis, R. L. G., Sousa, N. J. C., & Gimble, J. M. (2010). Adipose tissue derived stem cells secretome: soluble factors and their roles in regenerative medicine. *Current Stem Cell Research & Therapy*, *5*(2), 103–110. Retrieved from http://www.ncbi.nlm.nih.gov/pubmed/19941460

[69] Sarveazad, A., Babahajian, A., Bakhtiari, M., Soleimani, M., Behnam, B., Yari, A., … Joghataei, M. T. (2016). The combined application of human adipose derived stem cells and chon- droitinase ABC in treatment of a spinal cord injury model. *Neuropeptides*. https://doi.org/10.1016/j.npep.2016.07.004

[70] Snider, S., Cavalli, A., Colombo, F., Gallotti, A. L., Quattrini, A., Salvatore, L., … Mortini, P. (2016). *A novel composite type I collagen scaffold with micropatterned porosity regulates the entrance of phagocytes in a severe model of spinal cord injury*. 1–14. https://doi.org/10.1002/jbm.b.33645

[71] Sobajo, C., Behzad, F., Yuan, X.-F., & Bayat, A. (2008). Silk: a potential medium for tissue engineering. *Eplasty*, *8*, e47. Retrieved from http://www.ncbi.nlm.nih.gov/pubmed/18997857%0Ahttp://www.pubmedcentral.nih.gov/articlerender.fcgi?artid=PMC2567119

[72] Stevens, M. M., George, J. H., Stevens, M. M., & George, J. H. (2013). *Exploring and Engineering the Cell Surface Interface*. *1135*(2005). https://doi.org/10.1126/science.1106587

[73] Suzuki, M., Yasukawa, T., Mase, Y., Oyamatsu, D., Shiku, H., & Matsue, T. (2009). *Dielectrophoretic Micropatterning with Microparticle Monolayers Covalently Linked to Glass Surfaces - Langmuir (ACS Publications)*. (24), 11005–11011. Retrieved from http://pubs.acs.org/doi/full/10.1021/la048111p

[74] Thery, M. (2010). Micropatterning as a tool to decipher cell morphogenesis and functions. *Journal of Cell Science*, *123*(24), 4201–4213. https://doi.org/10.1242/jcs.075150

[75] Turcu, F., Tratsk-Nitz, K., Thanos, S., Schuhmann, W., & Heiduschka, P. (2003). Ink-jet printing for micropattern generation of laminin for neuronal adhesion. *Journal of Neuroscience Methods*, *131*(1–2), 141–148. https://doi.org/10.1016/j.jneumeth.2003.08.001

[76] Ude, A. U., Eshkoor, R. A., Zulkifili, R., Ariffin, A. K., Dzuraidah, A. W., & Azhari, C. H. (2014). Bombyx mori silk fibre and its composite: A review of contemporary developments. *Materials and Design*, *57*, 298–305. https://doi.org/10.1016/j.matdes.2013.12.052

[77] Varone, A., Knight, D., Lesage, S., Vollrath, F., Rajnicek, A. M., & Huang, W. (2017). The potential of Antheraea pernyi silk for spinal cord repair. *Scientific Reports*, 1–10. https://doi.org/10.1038/s41598-017-14280-5

[78] Vats, A., Tolley, N. S., Polak, J. M., & Gough, J. E. (2003). Scaffolds and biomaterials

for tissue engineering: A review of clinical applications. *Clinical Otolaryngology and Allied Sciences*, *28*(3), 165–172. https://doi.org/10.1046/j.1365-2273.2003.00686.x

[79] Vo, T. N., Kasper, F. K., & Mikos, A. G. (2012). Strategies for controlled delivery of growth factors and cells for bone regeneration. *Advanced Drug Delivery Reviews*, *64*(12), 1292–1309. https://doi.org/10.1016/j.addr.2012.01.016

[80] Wen-Wen, L., Zhen-Ling, C., & Xing-Yu, J. (2009). Methods for cell micropatterning on two-dimensional surfaces and their applications in biology. *Fenxi Huaxue/ Chinese Journal of Analytical Chemistry*, *37*(7), 943–949. https://doi.org/10.1016/S1872-2040(08)60113-9

[81] Wong, L., Pegan, J. D., Gabela-Zuniga, Basia, K., E., M., & McCloskey, K. (2017). Leaf-inspired Microcontact Printing Vascular Patterns. *Biofabrication*, *9*(021001). https://doi.org/10.1088/1758-5090/aa721d

[82] Xu, C., Lei, C., Meng, L., Wang, C., & Song, Y. (2012). *Review Article Chitosan as a barrier membrane material in periodontal tissue regeneration*. 1–9. https://doi.org/10.1002/jbm.b.32662

[83] Yu, B., Chou, P., Sun, Y., Lee, Y., & Young, T. (2006). *Topological micropatterned membranes and its effect on the morphology and growth of human mesenchymal stem cells (hMSCs)*. *273*, 31–37. https://doi.org/10.1016/j.memsci.2005.10.012

[84] Yuan, Y., Zhang, P., Yang, Y., Wang, X., & Gu, X. (2004). *The interaction of Schwann cells with chitosan membranes and fibers in vitro*. *25*, 4273–4278. https://doi.org/10.1016/j.biomaterials.2003.11.029

[85] Zarrintaj, P., Manouchehri, S., Ahmadi, Z., Saeb, M. R., Urbanska, A. M., Kaplan, D. L., & Mozafari, M. (2018). Agarose-based biomaterials for tissue engineering. *Carbohydrate Polymers*, *187*(114), 66–84. https://doi.org/10.1016/j.carbpol.2018.01.060

[86] Zhao, H. P., Feng, X. Q., Yu, S. W., Cui, W. Z., & Zou, F. Z. (2005). Mechanical properties of silkworm cocoons. *Polymer*, *46*(21), 9192–9201. https://doi.org/10.1016/j.polymer.2005.07.004

[87] Zheng, L., Jiang, J., Gui, J., Zhang, L., Liu, X., Sun, Y., & Fan, Y. (2018). Influence of Micropatterning on Human Periodontal Ligament Cells' Behavior. *Biophysical Journal*, *114*(8), 1988–2000. https://doi.org/10.1016/j.bpj.2018.02.041

APPENDIX

1. Complementary tables of the obtained data

a. Surface wettability and free energy

Samples	CA (º)		SFE (mN/m)			
	Water	MI	Eq. State	OWRK/Fawkes	Wu	Zisman
CTR	59.05 ± 8.27	34.05 ± 1.89	45.13 ± 2.44	53.29 ± 3.70	59.21 ± 3.60	37.49 ± 5.10
MP	70.31 ± 5.02	40.90 ± 9.28	41.23 ± 3.56	47.51 ± 5.72	53.31 ± 5.48	28.95 ± 13.54

The results of the SFE methods were calculated automatically by the OneAttension software, following the equations:

- Equation of state:

$$\cos\theta_Y = -1+2\sqrt{\frac{\gamma_{sv}}{\gamma_{lv}}}e^{-\beta(\gamma_{lv}-\gamma_{sv})^2} \quad (6)$$

- OWRK/Fawkes:

$$\gamma_{sl} = \gamma_{sv} + \gamma_{lv} - 2\sqrt{\gamma^{d}_{sv}\gamma^{d}_{lv}} - 2\sqrt{\gamma^{p}_{sv}\gamma^{p}_{lv}} \quad (7)$$

This equation can be combined with the Young equation (1) and be written as

$$\sqrt{\gamma^{d}_{sv}\gamma^{d}_{lv}} + \sqrt{\gamma^{p}_{sv}\gamma^{p}_{lv}} = 0.5\,\gamma_{lv}(1+\cos\theta_Y) \quad (8)$$

- Wu:

$$\gamma_{sl} = \gamma_{sv} + \gamma_{lv} - 4\left[\frac{\gamma^{d}_{sv}\gamma^{d}_{lv}}{(\gamma^{d}_{sv}+\gamma^{d}_{lv})} + \frac{\gamma^{p}_{sv}\gamma^{p}_{lv}}{(\gamma^{p}_{sv}+\gamma^{p}_{lv})}\right] \quad (9)$$

When combined with the Young equation (1), becomes

$$\left[\frac{\gamma^{d}_{sv}\gamma^{d}_{lv}}{(\gamma^{d}_{sv}+\gamma^{d}_{lv})} + \frac{\gamma^{p}_{sv}\gamma^{p}_{lv}}{(\gamma^{p}_{sv}+\gamma^{p}_{lv})}\right] = 0.25\gamma_{lv}(1+\cos\theta_Y) \quad (10)$$

In these equations: β is a coefficient, determined experimentally, related to the materials and equals 0,0001247; θ_Y is the contact angle (CA); γ_{lv} is the surface tension of the liquid; γ_{sl}

is the interfacial tension between solid and liquid; γ_{sv} is the surface free energy (SFE) of the solid; for γ^{d}_{sv} and γ^{p}_{sv}, d and p are the dispersive and polar components, respectively.

The Zisman method, however, is rather a plot and not an equation.

b. Thickness of the CTR and MP samples, dry or hydrated with PBS for 2 hours

Samples	CTR		MP	
	Dry	Hydrated	Dry	Hydrated
Thickness (mm)	0.03 ± 0.02	0.06 ± 0.02	0.07 ± 0.02	0.08 ± 0.01

The thickness increase tax (Δx) was calculated from:

$$\Delta x = \frac{x_{PBS\ hydrated} - x_{Dry}}{x_{Dry}} \times 100\% \quad (11)$$

c. Mechanical properties of both dry and PBS hydrated samples

Samples	CTR		MP	
Condition	Dry	Hydrated	Dry	Hydrated
Young's Modulus (MPa)	0.40 ± 0.24	0.17 ± 0.08	0.33 ± 0.09	0.09 ± 0.06
Ultimate Tensile Strength (Mpa)	4.70 ± 2.95	1.54 ± 0.48	2.74 ± 0.78	1.03±0.32
Strain @ Tensile Strength (%)	47.19 ± 27.74	13.22 ± 4.31	21.01 ± 11.14	20.77 ± 6.37
Stress @ Break (MPa)	4.51 ± 2.59	1.52 ± 0.47	2.44 ± 0.80	1.01 ± 0.32
Elongation @ Break (%)	48.56 ± 28.41	14.14 ± 4.33	25.17 ± 12.89	21.77 ± 6.58
Offset Yield Stress (MPa)	2.96 ± 1.82	1.18 ± 0.28	2.05 ± 0.78	0.55 ± 0.12
Strain Energy (MPa)	218.93 ± 215.95	28.13 ± 13.59	63.15 ± 38.74	19.60 ± 8.78

d. Cell quantification by immunostaining

Membrane	Cell Type	Samples	Cell Count
CTR	hASCs	1	310.00 ± 141.99
		2	142.00 ± 34.18
		3	342.00 ± 103.24
		4	110.33 ± 15.14
	hPDLs	1	550.00 ± 32.92
		2	535.00 ± 45.21
		3	501.00 ± 46.23
		4	509.00 ± 100.38
MP	hASCs	1	207.67 ± 92.18
		2	82.00 ± 25.98
		3	94.67 ± 9.86
		4	82.33 ± 8.08
	hPDLs	1	291.67 ± 72.73
		2	499.67 ± 447.39
		3	377.67 ± 231.95
		4	301.00 ± 92.00

e. Metabolic activity

Membrane	Cell Type	Samples	Metabolic Activity (at 490 nm)
CTR	hASCs	1	0.05 ± 0.01
		2	0.05 ± 0.00
		3	0.05 ± 0.00
		4	0.00 ± 0.00
	hPDLs	1	1.06 ± 0.06
		2	0.88 ± 0.01
		3	0.68 ± 0.01
		4	0.97 ± 0.01
MP	hASCs	1	0.10 ± 0.08
		2	0.03 ± 0.01
		3	0.00 ± 0.01
		4	-0.06 ± 0.00
	hPDLs	1	0.58 ± 0.05
		2	1.14 ± 0.04
		3	0.41 ± 0.02
		4	0.61 ± 0.07

The results on this table were obtained after the subtraction of the blank values.

2. Data acquired from the statistical analysis using IBM SPSS Statistics 24

a. Surface wettability and free energy

Table 1. Outcomes and p-values of the statistical analysis to the CA and SFE measurement results.

Tests (CTR Vs. MP)	CA	SFE (OWRK/Fowkes)
P Value	<0.01	0.04
Outcome	Different	Different

b. Thickness of the CTR and MP samples, dry or hydrated with PBS for 2 hours

Table 2. P value results from the statistical analysis to the thickness of either membrane type or hydration state.

Conditions	CTR Vs MP	Dry Vs Hydrated
P Value	< 0.01	0.09
Outcome	Different	Not Different

Table 3. P value results from the statistical analysis to the thickness of all sample groups.

Samples	CTR Dry	CTR Hydrated	MP Dry	MP Hydrated
CTR Dry	X	0.26	0.03 (Different)	0.01 (Different)
CTR Hydrated	0.26	X	0.66	0.31
MP Dry	0.03 (Different)	0.66	X	0.91
MP Hydrated	0.01 (Different)	0.31	0.91	X

c. Mechanical properties of both dry and PBS hydrated samples

Table 4. P value results from statistical analysis of the Young's modulus of either membrane type or hydration state.

Conditions	CTR Vs MP	Dry Vs Hydrated
P Value	0.24	<0.01
Outcome	Not Different	Different

Table 5. P value results from the statistical analysis to the Young's modulus of all sample groups.

Samples	CTR Dry	CTR Hydrated	MP Dry	MP Hydrated
CTR Dry	X	0.09	0.88	0.01(Different)
CTR Hydrated	0.09	X	0.30	0.76
MP Dry	0.88	0.30	X	0.06
MP Hydrated	0.01 (Different)	0.76	0.06	X

Table 6. P value results from statistical analysis of the ultimate tensile strength of either membrane type or hydration state.

Conditions	CTR Vs MP	Dry Vs Hydrated
P Value	0,09	<0,01
Outcome	Not Different	Different

Table 7. P value results from the statistical analysis to the ultimate tensile strength of all sample groups.

Samples	CTR Dry	CTR Hydrated	MP Dry	MP Hydrated
CTR Dry	X	0.03 (Different)	0.23	0.01 (Different)
CTR Hydrated	0.03 (Different)	X	0.62	0.95
MP Dry	0.23	0.62	X	0.34
MP Hydrated	0.01 (Different)	0.95	0.34	X

Table 8. P value results from statistical analysis of the elongation at break of either membrane type or hydration state.

Conditions	CTR Vs MP	Dry Vs Hydrated
P Value	0.29	0.02
Outcome	Not Different	Different

Table 9. P value results from the statistical analysis to the elongation at break of all sample groups.

Samples	CTR Dry	CTR Hydrated	MP Dry	MP Hydrated
CTR Dry	X	0.02 (Different)	0.14	0.08
CTR Hydrated	0.02 (Different)	X	0.70	0.88
MP Dry	0.14	0.70	X	0.99
MP Hydrated	0.08	0.88	0.99	X

d. Cell quantification by immunostaining

Table 10. P value results from statistical analysis of the cell count in either membrane type or cell type.

Conditions	CTR Vs MP	hASCs Vs hPDLs
P Value	< 0.01	< 0.01
Outcome	Different	Different

Table 11. P value results from the statistical analysis to the cell count in all sample groups.

Samples	CTR hASCs	CTR hPDLs	MP hASCs	MP hPDLs
CTR hASCs	X	<0.01 (Different)	0.29	0.12
CTR hPDLs	<0.01 (Different)	X	<0.01 (Different)	0.08
MP hASCs	0.29	<0.01 (Different)	X	<0.01 (Different)
MP hPDLs	0.12	0.08	<0.01(Different)	X

e. Metabolic activity

Table 12. P value results from statistical analysis of the metabolic activity in either membrane type or cell type.

Conditions	CTR Vs MP	hASCs Vs hPDLs
P Value	0.23	< 0.01
Outcome	Not Different	Different

Table 13. P value results from the statistical analysis to the metabolic activity in all sample groups.

Samples	CTR hASCs	CTR hPDLs	MP hASCs	MP hPDLs
CTR hASCs	X	<0.01 (Different)	1.00	<0.01 (Different)
CTR hPDLs	<0.01 (Different)	X	<0.01 (Different)	0.40
MP hASCs	1.00	<0.01 (Different)	X	<0.01 (Different)
MP hPDLs	<0.01 (Different)	0.40	<0.01(Different)	X